scientific reports

Check for updates

OPEN

Thixo-viscoelastoplastic rheological characterisation of human mucus using a multimode BMP constitutive equation approach

Michelle Figueroa-Landeta[1], Sarahí L. Esponda-Cervantes[1], M. Fernanda Reyes-Tenorio[1], Octavio Manero[2,3] & J. Esteban López-Aguilar[1,3]✉

In this work, the most recent Bautista-Manero-Puig (BMP) constitutive model-variant, i.e., the BMP+_τ_p rheological equation-of-state, is used as a theoretical approach to describe the thixo-viscoelastoplastic characteristics of human mucus-sputum in rheometric flows, focused on healthy, Cystic Fibrosis (CF) and Chronic Obstructive Pulmonary Disease (COPD) affected samples, to determine its mechanical-to-biological response interplay. The BMP+_τ_p model reproduces quantitatively the mucus-sputum rheological behaviour in steady and unsteady shearing flows under conventional protocols. From such theoretical characterisation, predictions are presented for LAOS and uniaxial extension, evidencing that thixotropy impacts strongly on sputum rheological behaviour. On plasticity and thixotropy, an explicit inverse relationship between a fluidisation stress and the BMP+_τ_p thixotropic parameters is found and tested against independent measurements, giving: (i) quantitative agreement with medical reports; and (ii) evidence of a highly non-linear internal-structure rearrangement under LAOS. In the scarcely-treated mucus-sputum extensional deformations, BMP+_τ_p predictions provide a rheological signature as augmented strain-hardening extensional-viscosity peaks: an additional source of flow-resistance in expectoration processes, with mixed shear-to-extensional flows. This may serve as: (i) an advanced rheological basis for biomarker development to determine the patient state, (ii) a tool for the efficacy-of-treatment evaluation with potential application for newly-emerging illnesses, e.g., COVID-19, closely-related with CF in sputum consistency and symptoms.

Keywords Human mucus-sputum rheology, Cystic fibrosis, COPD and COVID-19, Thixo-viscoelastoplasticity, Time-dependent yield stress and viscoelasticity, Extensional viscosity, Rheological basis for biomarker development

Mucus is a secretion that serves different functions for organs and glands in living systems, e.g., expelling of external micro-particles, hindering access of noxious agents to the epithelium and, in the respiratory tract, forming a selectively permeable layer for the diffusion and exchange of gases, and tissue lubrication[1]. Mucus composition consists of about 1% weight of salts or electrolytes, 0.5% - 1% of free proteins, 1% -5% mucin glycoproteins (mucins), and 97% water[2–4]. Also, bronchial mucus contains a significant proportion of lipids and, in pathological states, can also contain DNA and traces of other proteins coming from ruptured leukocytes[3]. Such composition confers non-Newtonian characteristics to mucus, particularly due to a somewhat complex protein-entanglement process[5], i.e., (i) in general, protein concentration increases viscosity; (ii) mucin covalent

[1]Facultad de Química - Faculty of Chemistry, Departamento de Ingeniería Química - Chemical Engineering Department, Universidad Nacional Autónoma de México - National Autonomous University of Mexico, Ciudad Universitaria, Coyoacán 04510, CDMX, México. [2]Instituto de Investigaciones en Materiales - Materials Research Institute, Universidad Nacional Autónoma de México - National Autonomous University of Mexico, Ciudad Universitaria, Coyoacán 04510, CDMX, México. [3]Institute of Non-Newtonian Fluid Mechanics, Faculty of Science and Engineering, Swansea University, Bay Campus, Fabian Way, SA1 8EN Swansea, West Glamorgan, United Kingdom. ✉email: jelopezaguilar@quimica.unam.mx

networked bonds confer mucus its viscoelastic properties[6,7]; (iii) mucin clusters strengthened by non-mucin proteins generate a finite yield stress[8,9]; and (iv) the three-dimensional structure of the protein network correlates with time-dependent rheological properties, such as thixotropy[10–12]. We encourage our readers to see a broader explanation of mucin network characteristics, evolution and factors modifying its rheological nature in the work of Georgiades et al.[13], Kavishvar & Ramachandran[9], Wagner et al.[14], and Esteban-Enjuto et al.[15,16] Consequently, any affectation upon such network will lead to different complex rheological responses, which may be broadly classified as thixo-viscoelastoplastic (TVEP)[8].

Mucus rheological characterisation may help to understand its role within the human body[5,11,17–20]. For example, respiratory mucociliary clearance relies on the rheological qualities of mucus, which modulate the transport processes between the cilia layers[21]. Furthermore, the rheological features of mucus may serve as biomarkers for respiratory disease diagnosis and monitoring[18], even as predictors for clinical outcomes[22–25], considering that respiratory diseases alter the usual concentration of proteins through antibody presence, strengthening the mucin network and changing the mucus flow properties[25]. However, sputum specimen collection (which is a mixture of saliva and mucus, coughed up from the respiratory tract) typically results in a non-invasive and straightforward procedure compared to obtaining mucus samples[26]. This is why most of research in the field of rheological characterisation is done upon sputum[5,11,17–19]. However, in some clinical settings, a more intensive approach may be necessary when patients have difficulty in expelling fluid from the upper respiratory tract[26].

Like any ideal biomarker, those based on rheometric measurements must be reproducible, clinically relevant, sensitive, reliable, and easy to obtain[27], aspects not yet fulfilled because of the lack of consensus on the experimental protocols and the pieces of information needed to understand and differentiate the complex rheological response of sputum. Nonetheless, rheological biomarkers present some advantages over conventional ones, such as being cost and time-efficient[17], even standing as a non-invasive alternative to predict clinical symptoms[22].

Two diseases whose study continues in the spotlight regarding their biomarker improvement are Chronic Obstructive Pulmonary Disease (COPD) and COVID-19[28,29]. According to the World Health Organization[30], one of the most common chronic respiratory diseases is COPD, which is the third leading cause of death worldwide. COPD symptoms include coughing, difficulty of breathing, wheezing, and tiredness, which leads to restricted airflow[30]. Besides, the lungs can get damaged or clogged with phlegm[30]. On the other hand, the COVID-19 disease has persisted as a worldwide health issue since the pandemic began and still calls for long term sustained prevention, controlling and management activities[9,31]. Severe Acute Respiratory Failure (SARS) is one of COVID-19 main complications. SARS is characterised by mucus hypersecretion and high viscosity sputum, resulting in chronic lung-clogging, inflammation and airway obstruction, accompanied with excessive bacterial growth and lack of proper oxygenation in the worst cases[17,32]. The flow properties of COVID-19 mucus are reported to be comparable in quality and intensity to those of Cystic Fibrosis (CF)[9]. Indeed, such intense growth of the sputum consistency is apparent in CF that its medical designation as *mucoviscidosis* reflects its critical condition of development[19]. Then, derived from the lack of recent studies reporting a thorough rheological characterisation of COVID-19 patients sputum - being, to the best of our knowledge, the work of Kratochvil et al.[9] the only one dealing with such rather new respiratory illness-, one way to explore the rheological response of COVID-19 sputum is to study CF samples instead.

In Table 1, the most common biomarkers for COPD and CF are summarised, emphasizing on the type of biomarker, its characteristics and its utility in determining illness-state and treatment, if applicable. Mostly, they serve to determine severity and prognosis of respiratory disease[33,34], to monitor the therapeutic response under specific treatments[35], and to determine the occurrence of disease exacerbations[36] (defined as a sustained worsening of symptoms, that has an acute onset and requires a change in the patients treatment[37]). Some of them are directly related to major symptoms, e.g. the Forced Expiratory Volume in one second (FEV_1), yet they are not exclusively used for either COPD or CF, but provide key information on the patient state, e.g., Clara cell protein (CC16)[38].

To date, there are several studies seeking to link the macroscopic flow properties of mucus and sputum with its physicochemical characteristics, as a way to develop biomarkers for COPD an CF.

Among those of *experimental character* in the field of rheological characterisation, the early work of Dawson et al.[5] attempted to describe human sputum as a viscoelastic solid, with a characteristic gel-like behaviour at small deformation amplitudes, where the storage modulus (G') rises monotonically, whilst the loss modulus (G'') remained constant over the frequency-range analysed. Under larger deformations, their sputum samples displayed thinning trends in viscosity and elastic modulus.

In this same context, Nielsen et al.[11] provided evidence of a more complex rheological response of sputum, for which significantly long times to attain steady-state viscosity measurements are reported, marking the influence of thixotropy in their sputum samples. Here, similarly to Dawson et al.[5], a significantly-increased *consistency* of CF sputum has been systematically associated with the presence of DNA and other proteins originating from ruptured-leukocyte remains - in excess when an infection is active in the human body.

More recently, Tomaiuolo et al.[17] concluded that the G' magnitude is correlated to the FEV_1 index and to specific bacterial colonies in CF-affected sputum samples. Thus, such rheometric G'-measurement helped to identify the disease severity, which was essentially related -according to these authors- to the presence of high molecular-weight components of sputum, which rendered their samples as thixo-viscoelastoplastic materials.

Hill et al.[34] proposed the mucus solid-concentration as a potential biomarker (considering solids as mucin and non-mucin proteins, salts, lipids, and cellular debris[40]). These authors were able to measure the differences between healthy, COPD and CF samples, finding a critical solid concentration at which a transition from liquid to solid-like response occurs, recorded using the calculated G' and G'' moduli magnitudes.

Nettle et al.[22] carried out Small Amplitude Oscillatory Shear (SAOS) and creep-recovery tests in an attempt to correlate the rheological properties of sputum with clinical data on the severity of symptoms in COPD patients.

Biomarker	Illness	Classification	Characteristics
Forced Expiratory Volume in 1 second (FEV_1)	COPD, CF	Severity and prognosis	Measures lung activity and air flow. Reduction, irreversibility and chronicity of the FEV_1 differentiate COPD and CF[33,34].
Exhaled Breath Condensate (EBC)	COPD	Exacerbations	Recollected by cooling exhaled air. pH of EBC from COPD patients is lower than that of healthy individuals, providing a biomarker based on the acidity of the breath condensate[27].
Neutrophils	COPD, CF	Exacerbations	These are inflammatory cells which activity serve to monitor lung function. They are related to airway obstruction, mucus hypersecretion and alveolar destruction.[35,36,39]
C-Reactive Protein (CRP)	COPD	Prognosis, mortality and exacerbations	This protein takes part on systematic inflammatory response. COPD patients present higher concentrations of CRP than healthy individuals[27,36].
Interleukin 6 (IL-6)	COPD	Exacerbations	This protein regulates the immunological response. COPD patients display higher IL-6 concentrations than healthy individuals[27,36].
Fibrinogen	COPD	Exacerbations	Predicts moderate and severe exacerbations in COPD, accompanied by an increment of concentration in inflammation phases[27,36].
Clara cell protein (CC16)	COPD	Severity and exacerbations	This protein possesses anti-inflammatory properties and its concentration decreases in COPD patients[27].
Surfactant Protein D (SP-D)	COPD	Therapeutic response	This protein protects against infections and oxidizing agents. COPD patients experiment relatively higher levels of SP-D and its concentration decreases when administrating corticosteroids[27].
Sweat-chloride concentration	CF	Therapeutic response	Reliable test for discriminating between minimal, partial and full CF transmembrane-conductance regulator (CFTR) protein function. Still needs clinical studies to support it as a biomarker for drug development[35].
Nasal Potential Difference (NPD)	CF	Therapeutic response	Isolates CFTR activity in nasal mucus and it is sensitive enough to detect dose-dependent bioactivity. Requires specialised equipment[35].
Intestinal Current Measurement (ICM)	CF	Therapeutic response	Tracks CFTR-dependent ion transport. Requires a rectal biopsy[35].
Bacterial density in sputum	CF	Therapeutic response	The most common bacteria linked to infection and morbidity on CF patients are P. aeruginosa, Burkholderia cepacia complex and Staphylococcus aureus. The presence of these bacteria is a sign of disease and it can be useful to determine the infection degree[35].

Table 1. Typical COPD and CF biomarkers.

Their findings suggested that the elastic modulus G' could be a more suitable measurement of mucus physical properties than the shear viscosity. These authors fitted their experimental elastic modulus data using the Power-Law constitutive relationship. Here, the Power-Law index was correlated with the ratio of FEV_1 to the Forced Vital Capacity of the lungs (FVC), namely FEV_1/FVC, which is a clinical measurement of COPD severity and a lung damage indicator[17,22]. Lower FEV_1/FVC, indicating the worst exacerbations, corresponded to smaller Power-Law indexes (all < 1), which is interpreted as a relatively more pronounced shear-thinning response.

Patarin et al.[19] characterised sputum samples from healthy individuals, asthma, COPD and CF patients in linear and non-linear viscoelastic regimes. They demonstrated how the sputum critical stress (σ_c), defined from the intersection between G' and G'' in an amplitude sweep, can be used to diagnose respiratory illnesses such as COPD and CF, since the ciliary transport efficiency declines with the augmentation of σ_c. In this respect, these authors provided representative measures of the elastic-modulus increase with the illness worsening, from which one can extract an increase of some 10-20 times the COPD-CF samples over the healthy references. For the plastic response measured through the critical stress, these authors reported distinct responses between COPD and CF-affected samples, and those of healthy individuals, for which an increase of some 5-10 units of stress is witnessed for the diseased samples. Therefore, their work highlights the importance of considering the dynamic properties of sputum as viable biomarkers for chronic bronchial diseases. In line with the work of Patarin et al.[19], Ghanem et al.[41] tested samples from healthy and CF patients with some illness degree and under a mucolytic spray treatment in simple shear flow, to evaluate the correlation between an apparent yield-stress and the illness development, for which the plastic properties of their samples turned out to be the best candidate for a biomarker development to monitor the mucolytic performance.

Jory et al.[20] used micro and macrorheology to quantify the viscoelastic properties of human bronchial epithelium mucus. Healthy and COPD samples were tested to obtain steady shear, frequency and deformation sweep curves. After fitting the data with the Power-Law rheological equation-of-state, they concluded that mucus behaves like a shear-thinning viscoelastic material at the macro-scale, and as a viscous liquid at the micro-scale. They explained this difference between macro and micro rheological responses by classifying mucus internal structure as an elastic filament network embedded in a soft gel, rendering sputum as a thixo-viscoelastic gel with yield stress that follows a Power-Law dependence under extreme shear-thinning regimes characterised by negative Power-Law indexes.

Kratochvil et al.[9] studied the physical, chemical and immunological properties of sputum infected with severe SARS-CoV-2. Here, these authors stated a direct relationship between the CF and COVID-19 sputum *consistency*. They identified a increased amount of DNA and hyaluronan (HA) in ill-secretion samples compared to healthy ones, which was reduced by an enzymatic treatment with HAdase and deoxyribonuclease. A comparison between the pre-treatment and post-treatment elastic modulus ($\Delta G_{Saline} - \Delta G_{Enzyme}$) revealed that this difference in consistency was almost null for healthy secretions, and different to zero for COVID-19-affected samples.

Despite of all these efforts, no agreement is found to date about what should be a suitable experimental protocol to obtain or test mucus and sputum samples[15]. Neither there is a standardised way to present nor interpret the rheometric measurements, partly given that flow properties vary form one patient to another regardless of their health condition[1], and that obtaining samples is challenging enough[10]. Additionally, most of experimental rheometry on mucus and sputum characterisation focus on shearing flow, since this kind of

deformation is hypothesised to dominate mucus propulsion in airways[20] during the mucociliary clearance process[42,43]. However, uniaxial extensional deformations, which play a relevant role in the mucus and sputum expectoration process - recall spasms and airway contraction-expansion in closure and opening processes[18,44,45]- remain unexplored, as well as their correlation with other material functions and complex flows occurring in the respiratory system.

In terms of *theoretical-rheological characterisation and computations*, López-Aguilar et al.[44] and Tabatabaei et al.[18] used early model-variants of the Bautista-Manero-Puig family-of-fluids, i.e., the NM_τ_p equation[46], and the Pom-Pom theoretical framework, to describe human COPD sputum and bile in biliary conducts with obstructions, and to simulate the formation of filaments and the biofluid response in obstructed conduits within the human body. Through such simulations it was possible to estimate the extensional viscosity evolution, and its influence in relevant physiological functions.

Erken et al.[47] employed a variant of the Saramito model, namely the Saramito-Herschel-Bulkley model, to fit the oscillatory shear experimental measurements reported by Patarin et al.[19]. The Saramito model is a combination of the Oldroyd-B and Bingham constitutive equations, whilst the Saramito-HB model is the corresponding Herschel-Bulkley variation[48,49]. The Saramito constitutive equation is characterised for physically-consistent predictions for G' in oscillatory-shear strain-amplitude sweeps, but not for G''. Saramito et al.[48,49] attempted to solve this problem by considering a kinematic-hardening mechanism. By comparison of the fitting parameters (elastic modulus, yield stress, Power-Law index and consistency parameter), Erken et al.[47] were able to set a clear difference between healthy, COPD, asthma and CF samples. The yield stress and elastic modulus of COPD and CF samples were ten times higher than those of healthy individuals, whilst G' magnitude of CF samples doubled the one from COPD patients. Erken et al.[47] also simulated the airway closure due to liquid plug formation; they concluded that this phenomenon is promoted and dominated by the mucus viscoelastic features.

Sedaghat et al.[43] have successfully approached the mucocilary clearance process by numerical simulation, using a multimode Giesekus equation. Such constitutive model was validated by Vasquez et al.[50] in steady and oscillatory shear flow, for a healthy mucus sample. However, this model does not account for time-dependent material responses, such as thixotropy, which appears clearly manifested in experiments[11]. Nevertheless, the results of Sedaghat et al.[43] prove that an Oldroyd-B-type multimode constitutive equation could be scalable to numerical simulations of physiological flows.

Applications - Monitoring clinical outcomes of targeted treatments for chronic pulmonary diseases. In general, the increase of viscosity and elastic modulus under chronic pulmonary diseases, which is often referred to as a *change in consistency*, is the distinctive trait between healthy and ill-mucus or sputum samples[9,51]. This explains to some extent the hindered mucus expectoration process, given that a stiffer consistency of mucus promotes chronic lung-airway obstruction, inflammation and infection[17]. Most basic treatments deal with these symptoms via the administration of active principles that lower the mucus viscosity or reduce its yield-stress[11]. Hence, a thorough rheological characterisation of sputum in healthy and relatively-advanced states of pulmonary illnesses could serve as a monitoring tool to determine the effectiveness of mucolytic treatments.

Other applications of such rheological characterisation are: (i) the prospective development *cheap and easy-to-use devices for clinical practise* in hospitals[17], (ii) *monitoring the effects of pharmacological treatments*, not only in humans[41] but also in the livestock and poultry industries[52], (iii) the study of *drug delivery* and *diffusion of active principles*[5,17], (iv) the study of illnesses for which the *rheological characterisation of biofluids* is relevant for diagnosis and treatment, such as periprosthetic joint infection and synovial fluid[23], eye edema, cataracts and vitreous humour[53], the reproductive system and vaginal fluids[54], among many others.

Hence, as it is evident in the richness of the afore-mentioned experimental and theoretical proposals alongside their applications, from a fundamental point-of-view, a deep study of the rheological response of mucus-sputum can contribute to shed light onto the changes in their micro-structure and their influence in the mucus-sputum macroscopic mechanical response and its effects in airway clearance[11].

Until now, we identify the following shortcomings for the rheological study of mucus an in the context of COPD and CF diseases: (1) the lack of a standardised protocol for interpreting rheometric measures; (2) the constitutive equations used to model the rheological phenomena of mucus are not able to capture all the range of mucus non-Newtonian responses (e.g. Power Law[20,22], Saramito[47], Quemada[12,21]), or are overly complex, compromising the capacity to using them in numerical simulations of physiological processes, such as the mucocilary clearance[43,50,55]; and (3) studies are constrained to rheometric shear flows. In this work, we propose a way to cope with these issues. Further than focusing on the elasto-plastic behaviour, we suggest that mucus thixotropic properties, that had been let aside in previous proposals[5,19,20,22], can provide valuable information to differentiate between healthy and ill samples. For this purpose, we use the most recent Bautista-Manero-Puig (BMP) constitutive equation model-variant, i.e., the BMP+_τ_p rheological equation-of-state[56–58], to describe the thixo-viscoelastoplastic response of healthy, COPD and CF mucus samples in rheometric flows, ranging from steady and transient shear, and oscillatory deformations. We contrast the model description against experimental data reported from literature[5,11,19,20]. With such capability of mathematical modelling prediction, we provide a consistent standardised framework to interpret the resulting flow properties in terms of the thixotropic and viscoelastic parameters of the BMP+_τ_p, including a measure of a critical stress for sample fluidisation, that identify starkly healthy-to-ill conditions of COPD and CF human mucus-sputum samples. From here, we provide numerical predictions for uniaxial extensional flow in the form of extensional viscosity trends in steady and transient tests, for which the BMP+_τ_p thixotropic parameters provide a signature of CF illness worsening.

Methods

To understand the mechanical response of any fluid through its rheological characterisation, it is essential to identify its non-Newtonian features to choose a suitable theoretical framework, which shall include a constitutive

equation relevant to the desired applications, capable of predicting the rheological features of the material[59,60]. In this section, we describe our characterisation methodology, which consists of three basic steps: (i) the selection of experimental data and its classification according to the rheological behaviour of samples displayed in their flow-curves, followed by (ii) the choice of a theoretical framework and its corresponding constitutive equation, potentially capable of reproducing the rheological features of the material; and (iii) the mathematical modelling of relevant rheometric tests.

Experimental data sets

Complex fluids such as human mucus and sputum show a wide range of rheological features that are not always observed unless more than one rheometric test is performed. In general, through steady shear flow tests, it is possible to identify shear thinning or thickening, and yield stress. Small and Large Amplitude Oscillatory Shear (SAOS and LAOS, respectively) data, such as frequency and amplitude sweeps, provide crucial information to classify viscoelastic and other non-linear responses[61–64]. Extensional flows can provide rheological fingerprints that are not present in shearing deformations, like, e.g., the Trouton ratio (Tr), which is a comparison between the fluid response to a strong deformation (in the sense of having a null vorticity tensor associated to the deformation) such as uniaxial extension, and its response to a shearing flow. Under uniaxial extension, a value of $Tr > 3$ indicates a viscoelastic strain-hardening response, that also can be anticipated from the increase in extensional viscosity from the first Newtonian plateau[60]. This is a manifestation of the additional resistance to flow biofluids might display in complex-flow configurations (e.g., in the airways), originating from its extensional rheological properties.[18] Transient tests, like thixotropic cycles, as well as step-up or step-down in shear rate or stress, and hysteresis loops, assess thixotropy and other time-dependent phenomena. For the characterisation of complex fluids, the more rheometric information available, the more complete the fluid description will be attained.

In the case of rheological characterisation of human sputum, several authors have dealt with this challenging experimental task[5,9,11,17,19,20,22,34,47,50]. As a *first step in this procedure*, we have selected a subset of experimental data reporting thoroughly the rheological response of human sputum under healthy and in some illness conditions, such as CF and COPD[5,11,17,19,20], which are listed in Table 2. This selection is based on the completeness of experimental protocols employed by the authors of these studies, and the availability of sufficient cases for comparison between healthy references, CF or COPD samples.

Here, the notion of *completeness* and *sufficiency* is related to the mathematical modelling of rheological responses of such complex biofluids, where choosing an appropriate or sufficient set of rheometric measurements is an important task to complete, since the amount of data sets and their quality will influence centrally the effectiveness of the fitting procedure and the corresponding rheological explanation that may be withdrawn. Depending on the complexity of the constitutive model, and particularly on the number of parameters in its formulation, one can set a minimum number of rheological signals to work with consistently. In terms of a thixo-viscoelastoplastic material such as sputum and mucus, rheological data sets providing information on the shear thinning characteristics of the biofluid plus its viscous Newtonian plateaux, a viscoelastic signal for determining the relaxation time, and a couple of signals of non-linear nature to find estimates for the thixotropic and plastic features would be enough to start with. If, on top of that, we had information on extensional response of these biofluids, we would be in an ideal scenario. Given that this is not the case, we propose our methodology and results as a starting point for a consistent rheological characterisation of these complex biofluids, with the potential to be expanded into a more detailed description provided that enough data sets on different composition, illness type and other relevant factors are available.

In view of the characteristics of the experimental protocols found in literature, which are based on shearing flow tests[5,11,17,19,20], and that to the best of our knowledge, the only extensional rheometric measurements available in the literature are performed upon mucin solutions and saliva, which are the simplest yet the closest systems to mucus and sputum[65,66], our results in the modelling of extensional flow are predictive in nature (see the Results and Discussion section). Then, their validity relies only on the hypothesis that if we can accurately describe the shearing flow phenomenology, through informed fittings under linear and non-linear regimes, it is likely that our predictions in other deformations, such as uniaxial extension, may offer insights into the response of mucus and sputum under such deformations. Moreover, it is important to provide predictive information on the extensional response of these biofluids, since its key role is well known in lung and airway blockage.[18,47,67,68]

	Healthy	CF	COPD
Jory et al.[20]	Healthy-1		COPD-1
Patarin et al.[19]	Healthy-2	CF-2	COPD-2
Nielsen et al.[11]		CF-3	
Dawson et al.[5]		CF-4	
Tomaiuolo et al.[17]		CF-5	

Table 2. Subset of studies reporting the rheometric characterisation for healthy, CF and COPD-affected sputum. Sample classification: In this work, each piece of information is identified by a different tag, according with the authors and disease. Healthy-1 (AM-J19 in the original work of Jory et al.[20]) and COPD-1 (RM-J17, likewise); Healthy-2, CF-2 and COPD-2 from the work of Patarin et al.[19]; CF-3 being the control sample in the original work of Nielsen et al.[11]; CF-4 from Dawson et al.[5], and CF-5 account for all the samples analysed by Tomaiuolo et al.[17], i.e. CF mild, severe and very severe.

	η vs $\dot{\gamma}$	G',G'' vs ω	G',G'' vs γ	Lissajous	η vs t	J vs t	γ vs t	Hysteresis
Healthy	Healthy-1	Healthy-1	Healthy-1	Healthy-1			Healthy-1	
		Healthy-2	Healthy-2					
CF		CF-2	CF-2					
	CF-3	CF-3	CF-3		CF-3	CF-3		CF-3
	CF-4	CF-4	CF-4					
	CF-5	CF-5						CF-5
COPD	COPD-1	COPD-1	COPD-1	COPD-1				
		COPD-2	COPD-2					

Table 3. Subset of studies reporting the rheometric characterisation for healthy, CF and COPD-affected sputum. Classification according to experimental protocol followed. The symbol η represents apparent viscosity, $\dot{\gamma}$ is the shear rate, ω is the frequency of deformation (oscillatory shear), γ is the strain (for steady and oscillatory shear), and J symbolises the compliance.

Author	Experimental protocol	Main findings
Jory et al.[20]	Mucus samples were collected from bronchialepithelial cells cultures that were obtained through biopsy from 17 healthy individuals, smokers and COPD patients. The samples were stored at $4^{\circ}C$ before being tested at $20^{\circ}C$ in cone/plate AntonPaar MCR 502 and MCR 30 rheometers.	Extreme shear-thinning behaviour was observed in all samples. Evidence of a yield stress was found and amounted in the range of 0.05-0.2 Pa.
Patarin et al.[19]	Mucus samples from 45 individuals (healthy and asthma, COPD and CF patients) were obtained by voluntary and induced expectoration. Saliva was removed from the samples. Rheological measurements were performed at $37^{\circ}C$ with *Rheomuco*, a strain-controlled oscillatory rheometer.	The measurements allowed to distinguish the effects obstructive diseases (CF and COPD) have on mucus samples, contrasting the critical stress σ_c-values associated to each type of sample, i.e., 5-10 Pa for obstructive diseases, whilst non-obstructive affections display 1 Pa for healthy and asthma. G' magnitude at the linear viscoelastic regime (LVE) increases with disease severity in consistency with FEV_1 values for each case.
Nielsen et al.[11]	Sputum samples were obtained from 23 CF patients and stored at $-20^{\circ}C$ for up to six months. Rheometric tests were performed at $25^{\circ}C$, using strain-controlled rheometers, i.e., Bohlin VOR (parallel plate geometry), RFS-II instruments (cone-plate fixture), and Haake RS100 (parallel plate geometry).	The authors found that mucus is a viscoelastic fluid with multiple relaxation times and thixotropic behaviour, dominated by inter and intramolecular interactions. They concluded that measurements of elastic moduli, rather than viscosity, are closely related to the mechanical properties of sputum in situ.
Dawson et al.[5]	Samples from CF patients were obtained by induced expectoration, and analysed immediately after their extraction. Measurements were carried out with a cone-plate strain-controlled ARES-100 rheometer.	The viscoelasticity of mucus mainly stems from the interactions between its macromolecular components, rather than from their concentration. Particle transport inside the mucus layer in the lungs is delayed and even arrested by the viscoelastic nature of mucus.
Tomaiuolo et al.[17]	Sputum samples from 33 CF patients were collected and classified by type of bacterial colonisation and disease severity (FEV_1). The samples were tested at room temperature with a controlled-stress rheometer, using a cone-plate fixture.	The authors concluded that G' has a strong correlation with bacterial colonisation and FEV_1 values, so it can be used instead of conventional biomarkers.

Table 4. Subset of studies reporting the rheometric characterisation for healthy, CF and COPD-affected sputum - Particularities across experimental studies are provided.

Returning to the experimental data sets, in order to summarise and classify our selection to be considered in this work, the type of samples and experimental protocols reported in the literature are listed in Tables 3 and 4. We prioritised studies comprising material functions for steady flows, oscillatory shear and transient tests. Table 3 serves to classify the sample type, either Healthy, CF or COPD affected, according to the rheological property explored. Here, the more common material properties studied are steady simple-shear apparent viscosity η against $\dot{\gamma}$, and storage G' and loss G'' moduli response under oscillatory shear, observing frequency ω and deformation-amplitude γ variations. The more advanced and detailed inspection of sputum samples are performed by Jory et al.[20], Nielsen et al.[11], Dawson et al.[5], and Tomaiuolo et al.[17], under Lissajous curves obtained under LAOS protocols, transient viscosity, compliance and deformation responses to uncover the thixotropic features of human sputum. In literature, the general practice is to report only representative experimental results. Therefore, the mathematical modelling presented in this paper is based on that average data.

In addition, Table 4 provides a brief description of the rheological measurements, the flow characteristics reported by those authors and its relationship with their clinical use, where applicable. This summary may serve to condensate and identify the main rheological characteristics of human sputum. From this data collection, we analysed the experimental results (see Tables 3 and 4), from which we start by making reference to specific pieces of information in the afore-mentioned references to signal and identify key rheological responses:

(i) *Apparent viscosity response* - In Fig. 1 of the work of Jory et al.[20], as well as in Fig. 7 in Nielsen et al.[11], in Fig. 1c in Dawson et al.[5], and in Fig. 1a on Tomaiuolo et al.[17], a *marked shear-thinning response* of mucus is revealed through a flow curve (viscosity versus shear-rate) for which the viscosity drops with shear-rate increase some five-to-seven orders-of-magnitude. Moreover, such starkly marked shear-thinning trend follows a Power-Law-like trend with negative indexes of around -0.85 units, as reported by Jory et al.[20]. These two characteristics of mucus and sputum rheological response have already been reported for the flow of wormlike micellar solutions, where such negative Power-law indexes are signatures of the onset of a shear-banding instability. Shear banding is a flow transition characterised by a spontaneous segregation

of the fluid into bands of different material properties, e.g., viscosity or elastic moduli, and that has been described and systematically predicted with the BMP family-of-fluids[58].

(ii) *Storage G' and loss G'' moduli and yield stress* - Frequency sweeps under SAOS from Fig. 2 in Jory et al.[20], Fig. 1a in Dawson et al.[5], and Fig. 3 in Tomaiuolo et al.[17], unveil a viscoelastic response of soft-gel-like systems and yielding fluids under oscillatory deformation[69], as $G' > G''$ for low-to-moderate values of frequency (ω) and strain (γ). The supplementary material given by Jory et al.[20] and Fig. 1 in Patarin et al.[19] show that mucus response to oscillatory shear (G' and G'' versus strain) fits the classification of viscoelastic strain-thinning, according to the general convention: decreasing G' and G'' at high strain values, without overshoots for none of the moduli[62,70]. Also, following one of the methods to determine the existence of a yield stress in soft-gel-like systems, i.e. the point at which $G' = G''$[71], mucus samples manifest a measure of its plasticity, the so-called critical stress (σ_c).

(iii) *Thixotropy* - Evidence of mucus thixotropic behaviour is found in Fig. 4 and 5 in Nielsen et al.[11], and Fig. 1c in Tomaiuolo et al.[17], for which CF-sample flow curves display hysteresis (a common manifestation of thixotropy[72,73]), and the transient response in start-up flow test reflect the effect that the history-of-deformation has on the microstructure[11].

Hence, in culmination of *the first step of our proposed rheological-characterisation procedure*, this number of distinct rheological features permits to *qualify human sputum under healthy, and CF or COPD ill-conditions, as a thixo-viscoelastoplastic material.*

The *second step in our characterisation procedure* is to *choose a suitable theoretical framework and its relevant constitutive equation*, capable of describing the basic rheological features of the material at hand. In the present case, given that human sputum displays time-dependent viscoelastic features with marked yield-stress characteristics, the BMP constitutive modelling approach[56–58] arises as a feasible choice. The BMP family-of-fluids appears as a well-established option providing thixo-viscoelastoplastic responses, which have been tested in many different materials, such as thixo-viscoelastic wormlike micellar surfactant solutions[46,74], biofluids[18], aluminium alloys[75], among others. In this work, we use the most recent BMP constitutive equation model-variant: the BMP+_τ_p rheological equation-of-state[56–58].

Once chosen the theoretical framework to work with, the *third step in our characterisation protocol* comes with the *mathematical modelling of the relevant rheometric tests to characterise the material*. The results of such mathematical modelling are provided in the next section. Before presenting the experimental-to-theoretical comparison of sputum rheology and the corresponding predictions, we describe the BMP+_τ_p model in detail, alongside its qualities and advantages compared against other thixo-viscoelastoplastic rheological models in the literature, and the parameter-fitting procedure followed in this work.

The Bautista-Manero-Puig constitutive equation

The Bautista-Manero-Puig (BMP) rheological equation-of-state was proposed originally for describing the behaviour of worm-like micellar solutions[74,76]. The most recent version of this model, the BMP+_τ_p rheological equation-of-state[56–58], considers some generalisations for the application of this model in complex flows, retaining its capabilities in terms of the prediction of shear-thinning, extension hardening and softening, highly non-linear viscoelasticity, and flow segregation in the form of apparent yield-stress and banding. Such generalisation is achieved via the inclusion of viscoelasticity into the material-structure time-evolution dynamics, and using the magnitude of the energy dissipated by the solute in motion to drive non-linear rheological responses - for further details, refer to López-Aguilar et al.[56–58].

The mathematical formulation of the BMP+_τ_p model consists of stress ($\boldsymbol{\tau}$) contributions expressed in an additive fashion, conceptualising the behaviour of a dissolution under an Elastic-Viscous Stress-Splitting approach in a generalised Oldroyd-B-like differential formulation, composed by an upper-convected Maxwell component for the solute, symbolised as $\boldsymbol{\tau}_p$, and a Newtonian contribution for the solvent, identified as $\boldsymbol{\tau}_s$, viz.:

$$f\boldsymbol{\tau}_p + \lambda_1 \overset{\nabla}{\boldsymbol{\tau}}_p = 2\eta_{p_0}\mathrm{D}, \tag{1}$$

$$\boldsymbol{\tau}_s = 2\eta_s\mathrm{D}, \tag{2}$$

where $\overset{\nabla}{\boldsymbol{\tau}}_p = \frac{d\boldsymbol{\tau}_p}{dt} + \mathrm{v}\cdot\nabla\boldsymbol{\tau}_p - \nabla\mathrm{v}^T\cdot\boldsymbol{\tau}_p - \boldsymbol{\tau}\cdot\nabla\mathrm{v}$ defines the upper-convected time-derivative of $\boldsymbol{\tau}_p$. The viscoelastic relaxation-time λ_1 modulates the influence of this upper-convected time derivative and, hence, the strength of viscoelasticity of the material. The diffusive mechanisms on both solute and solvent stress components are modulated by η_{p_0} and η_s, respectively, which, correspondingly, represent the level of the solute first-Newtonian plateau and the solvent viscosity. Here, the gradient operator ∇ applies over the spatial coordinates and the superscript ^{T} stands for a transpose operation over the velocity-gradient tensor $\nabla\boldsymbol{v}$. The rate-of-deformation tensor $\boldsymbol{D} = \frac{1}{2}(\nabla\boldsymbol{v} + \nabla\boldsymbol{v}^T)$ collects the isotropic rates of deformation an element of fluid can experience in a three-dimensional space.

The solute stress equation (Eq.(1)) is coupled with a kinetic equation that describes the material internal-structure temporal evolution via a dimensionless fluidity measure (f), given by:

$$\left(\frac{\partial}{\partial t} + \mathrm{v}\cdot\nabla\right) f = \frac{1}{\lambda_s}(1-f) + k\left(\frac{\eta_{p_0}}{\eta_\infty + \delta} - f\right)|\boldsymbol{\tau_p} : \mathrm{D}|. \tag{3}$$

Here, f is defined as $f = \frac{\eta_{p_0}}{\eta_p}$, where η_p is the non-Newtonian viscosity of the solute; the total viscosity of the dissolution η is defined as $\eta = \eta_p + \eta_s$. The structure evolution equation describes the thixotropic properties of the material through a characteristic time of structure-construction λ_s, and the inverse of the structure-destruction stress k. These two mechanisms of structure construction and destruction obey a dynamical equilibrium in which the energy dissipated by the solute in motion drives the structure evolution in-between two extreme values: (i) $\eta_{p_0} + \eta_s$ for fully-structured materials, and (ii) $(\eta_\infty + \delta) + \eta_s$ for fully-unstructured fluid responses, where η_∞ is the non-Newtonian high shear-rate viscosity.

For flow-segregation response predictions in this context, the destruction coefficient k should take a linear functionality with the applied shear-rate of the form $k = k_0 + \nu\dot{\gamma}$;[58] here, ν is the shear-banding intensity-parameter. The quantities λ_s and k_0 implicitly depend on the fluid microstructure construction-destruction mechanisms[74]. Additionally, flow segregation in the form of yield-stress is obtained under extreme solute concentrations (translated as well into strong shear-thinning responses, or, low solvent-fraction β-conditions, i.e. $\beta = \frac{\eta_s}{\eta_{p_0}+\eta_s} << 1$. The viscoelastic contributions are significant if $\lambda_s << \lambda_1$.

The multimode version of the BMP+_τ_p equations follows as:

$$\boldsymbol{\tau} = \sum_{1}^{n} \boldsymbol{\tau}_p^n + \boldsymbol{\tau}_s, \tag{4}$$

where $\boldsymbol{\tau}_p$ and $\boldsymbol{\tau}_s$ obey Eq.(1) and n represents the number of stress modes considered.

As such, the BMP+_τ_p constitutive equation arises as a suitable theoretical framework to reproduce the mucus and sputum rheological responses based on the qualities of its precursor, the BMP model, as it can describe non-linear rheological responses in transient loops and small amplitude oscillatory shear (SAOS)[76]. Furthermore, a multi-mode version of the BMP equation successfully modelled the rheological behaviour of blood with various cholesterol levels[77]. Even later modifications of the BMP model reproduce qualitatively the response of thixotropic and viscoelastoplastic fluids in complex flows[56–58].

One of the main advantages of the BMP constitutive model is its simplicity: alongside the several rheological responses that it can describe, all its parameters have a specific physical-rheological meaning. Moreover, the BMP+_τ_p measure of yield stress may be described as *apparent*, since its definition depends on the relative difference between η_{p_0} and η_∞. Notably, it is possible to define a critical stress $\tau_c = \sqrt{\frac{\eta_\infty}{\lambda_s k_0}}$, which is analogue to the yield-stress in the Bingham model. τ_c can be identified in a τ_{12} vs $\dot{\gamma}$ log-log plot, as the plateau in shear stress[74].

Fitting procedure

There are three fundamental aspects of the mathematical modelling of rheological responses that lead to exploit the full describing ability of a constitutive equation. Firstly, one should know the significance of constitutive-model parameters and the physical meaning associated to their combinations. Secondly, one should determine the scope of rheological responses that can be predicted with the constitutive model chosen, by performing a parameter-sensitivity analysis. Finally, one should identify the role the parameters play under specific rheometric test aimed to determine the relevant material properties or generalised flow conditions. The meaning, sensitivity, and the role the parameters play on the predictions depend on the constitutive model characteristics and the kinematics imposed by the flow itself. Besides, understanding the theoretical model in the context of a multi-mode approach is key for analysing data coming from biological samples, since their characteristics are influenced by averaged effects coming from the inhomogeneous biofluid features.

As exposed in the previous section, in the specific case of our BMP+_τ_p model, its mathematical statement is engineered through two solute viscosity levels determined at vanishing and large deformation rates (η_{p_0} and η_∞ respectively), and the viscosity of the solvent contribution (η_s), which collapse in a single solvent-fraction parameter $\beta = \frac{\eta_s}{\eta_{p_0}+\eta_s}$; one parameter related to viscoelasticity (defined either as either λ_1 or G_0), two parameters related to internal-structure re-arrangement and thixotropy (λ_s and k_0), and a parameter for shear banding (ν). One can define a parameter to estimate the apparent yield-stress features of the sample, which linked to the calculated critical stress of fluidisation (τ_c) and is a combination of the thixotropic and viscous parameters. Hence, for this case, the BMP+_τ_p model has seven parameters to be determined.

Then, under transient homogeneous deformations, the mathematical nature of this problem arises as a system of ordinary differential equations for shear and normal stresses, fluidity, and moduli, with six unknowns per mode, for which a numerical algorithm based on a fourth-order Runge-Kutta method was used, and a Romberg integration scheme to calculate material functions for oscillatory shear tests.

In this kind of mathematical modelling exercises, in which the determination of model parameters associated with material functions is performed, care must be taken in the balance between the number of parameters to be determined (associated with the constitutive model complexity), and the quantity, quality, and type of experimental data-sets. Ideally, the number of parameters to be determined and the number of experimental data-sets should be equal, rendering a null number of *degrees-of-freedom*; if this condition is met, one can qualify the case as a *closed system*. In addition, experimental data sets need to come from appropriate protocols directed to identify specific rheological responses. An additional source of information on the magnitude of parameters may come from reports elsewhere; nevertheless, although such sources of informed estimations are convenient, sometimes they are scarce or not generally applicable, such as in the case of biofluids[1,8,15,16,78]. Complementarily, through a parameter-sensitivity analysis, it is possible to estimate the influence and values for the remaining unknown parameters. Further details on how the parameter combination and variation impact on the type of BMP+_τ_p responses are provided in the Appendix.

This generalised procedure applied to the BMP+_τ_p model crystallises over the next steps:

(i) *Steady-state viscosity against shear-rate flow curves* - From the experimental steady-state apparent viscosity response, one can extract the value of η_{p0}, η_∞, and the product of the thixotropic parameters $\lambda_s \cdot k_0$, which modulates the shear-thinning slope in the apparent viscosity response, and its inverse value provides the energy dissipation rate per unit volume necessary to breakdown the fluid internal structure. As it will be explained further in the following section, such an energy-dissipation measure correlates with the thixo-viscoelastoplastic rheological response of healthy and ill-conditioned human mucus-sputum. The product $\lambda_s \cdot k_0$, as well as η_{p0}, η_∞ values are kept fixed for the following fitting steps in this procedure, leaving only three unknowns per mode.

(ii) *Small Amplitude Oscillatory Shear flow* - These oscillatory shear results are used to find the number of stress-modes *n* needed to characterise the samples and the corresponding values of λ_1, related to viscoelastic features. Likewise, λ_1 spectra are kept fixed for the following steps, leaving only two parameters to determine per mode.

(iii) *Transient start-up shearing flows, Lissajous curves and thixotropic-loops* - Time-dependent tests in the form of start-up flows, Lissajous curves and thixotropic loops serve to determine the individual values of λ_s and k_0. Particularly, if there are both transient data and Lissajous curves available, it is possible to identify if a shear banding parameter is needed. This leaves only one parameter to be determined per mode.

(iv) *Viscosity of the Newtonian solvent* - Based on its physical meaning, we set η_s as the viscosity of water (the actual *solvent* of mucus[2,3]), which amounts 0.001 Pa s.

(v) *Closed systems* - The only closed system we are working with is CF-3[11]. Closure on the rest of systems is achieved by estimating parameter values observing trends in the closed systems.

Since one of our goals is to determine the generalised mechanical behaviour of mucus-sputum by using a TVEP theoretical approach in the characterisation of mucus and sputum, we considered finding the value of parameters through educated guesses and a trial-and-error procedure, supported by the parameter sensitivity analysis, to be acceptable enough in this instalment. The accuracy of the procedure is quantified through the R^2-coefficients reported. Notably, our results are quantitatively consistent with experimental values reported in the literature on typical measures used clinically[1,8,15,16,20,78], such as the fluidisation stress in the determination of a patient illness state, as we will discuss in the Results and Discussion section.

A final consideration in this procedure is relevant in this case, in which complex biological fluids are studied: a case-by-case analysis should be taken into account given that every study in Table 4 follows a different protocol for the collection and handling of samples. Additionally, as any thixotropic fluid, human sputum is sensitive to the deformation history[11,17]. Hence, the results presented in the Results and Discussion section are analysed by case-study following the organisation in Table 2.

Results and discussion

In this section, we show and discuss the results of the BMP+_τ_p experimental data fitting obtained under varied shear-deformation-based tests, and the predictions of this constitutive equation in uniaxial extensional deformations. These fittings are performed over the rheological characterisation protocols available in the literature, as summarized in Table 3. It is worthy to state that the analysis of these results is primarily addressed on the parameters of the first stress-mode, since this mode dominates the rheological responses in the linear and incipient non-linear regime, in which the physiological flow conditions within the airways occur, i.e., creeping flow conditions[42]. Additionally, parameters related to the first mode strongly influence the overall behaviour at medium and high deformation rates. Then, in our analysis we will be referring to the parameters of the first mode of stress response, unless otherwise stated.

In addition and contrast to previous studies[5,11,17,19,20,47], once a proper rheological characterisation is achieved under shearing deformations, predictions are provided on the response of each mucus-sputum case under uniaxial extensional flow, for which steady extensional viscosity η_E and transient material functions (tensile growth coefficient, η_E^+) are calculated. The extensional response of mucus and sputum is relevant to the expectoration process, in which extensional deformations prevail[18].

Following Table 2, result description is categorised according to each data-set with two main objectives: (i) to describe each data-set on its own context in terms of group-of-individuals tested and particular rheometric techniques used, to extract the specific rheological response of each data-set; (ii) then, with the characterisation of each sample, to find a generalised description of the rheological response of mucus and sputum in healthy and ill conditions.

Contrasting healthy and COPD samples through rheological characterisation (Healthy-1 and COPD-1 from Jory et al.[20])

Figure 1 provides the comparison between experimental data of steady simple shear flow reported by Jory et al.[20] and the fitting obtained under the BMP+_τ_p model. Note that experimental data is tagged according to the classification in Table 2. The apparent shear viscosity (η) against shear rate ($\dot{\gamma}$) plots in Fig. 1 show quantitative agreement between the model predictions and experimental data ($R^2 \geq 0.97$). Both healthy and COPD-affected mucus samples display a plastic response through an apparent yield stress, i.e., a drastic drop in viscosity from the first to the second Newtonian plateau[79]. From Table 5, one can gather that the level of the first Newtonian plateau ($\sum \eta_{p_0}^i + \eta_s$) for sample COPD-1 is almost three-times larger than that for Healthy-1, whilst the level of the second Newtonian plateau measured from the solute contribution ($\sum \eta_\infty^i + \eta_s$) in the case of COPD-1, double the one for sample Healthy-1. This phenomenon may be explained physiologically through the difference

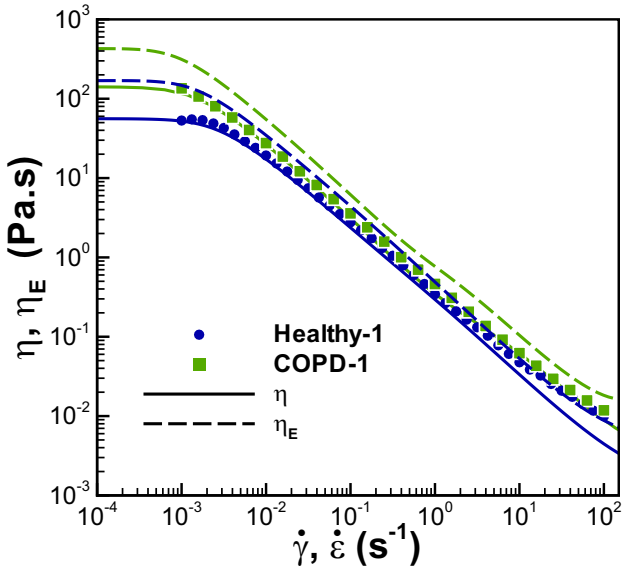

Fig. 1. Comparison between samples Healthy-1 and COPD-1 in simple shear: BMP+_τ_p-model predictions versus experimental data by Jory et al.[20]. See fitting parameters in Table 5. R^2(Healthy-1)$= 0.97$, R^2(COPD-1)$= 0.99$.

Parameter	Mode 1	Mode 2	Mode 3	Mode 4
Healthy-1				
η_{p0} (Pa.s)	55.0	0.90	0.10	0.03
η_∞ (Pa.s)	1.0^{-4}	$7.0x10^{-5}$	$1.0x10^{-4}$	$1x10^{-4}$
λ_1 (s)	80.0	2.0	0.25	$1.0x10^{-3}$
$\lambda_s * k_0$ (Pa^{-1}s)	$3.2x10^{-3}$	0.04	0.05	0.05
τ_c (Pa)	**0.18**	0.04	0.04	0.04
COPD-1				
η_{p0} (Pa.s)	140.0	1.2	0.1	$3.0x10^{-2}$
η_∞ (Pa.s)	$1.5x10^{-4}$	$5.0x10^{-5}$	$8.0x10^{-4}$	$8.0x10^{-4}$
$\lambda_1(s)$	160.0	2.0	0.2	$1.0x10^{-3}$
$\lambda_s * k_0$ (Pa^{-1}s)	$1.9x10^{-3}$	0.02	$6.0x10^{-3}$	0.01
ν (s)	1.5	0.0	0.0	0.0
τ_c (Pa)	**0.28**	0.05	0.36	0.28

Table 5. Fitting parameters for Healthy-1 and COPD-1 samples. Experimental data by Jory et al.[20].

in solid concentration, for which COPD-samples generally present an augmented quantity of DNA and other proteins coming from protective mechanisms.

With respect to the strength of the shear-thinning characteristics of both samples, one notes that they share the same order-of-magnitude drop in viscosity (a drop of some four-to-five decades in viscosity), and even a similar shear-thinning slope; within the BMP theoretical framework at hand, the value of the $\lambda_s \cdot k_0$ product determines such a rheological feature. The $\lambda_s \cdot k_0$ parameter-product has units of inverse of rate of energy-dissipation per unit volume; hence, $(\frac{1}{\lambda_s \cdot k_0})$ represents the characteristic energy dissipation rate per unit volume required to breakdown the fluid structure. Here, from Table 5, one notes that $\lambda_s \cdot k_0$ product across samples appears under the same order-of-magnitude, but smaller in the case of sample COPD-1; in general, the reduction of $\lambda_s k_0$ in the BMP+_τ_p renders a weaker shear-thinning response, which correlates with the augmentation of viscosity for sample COPD-1. In this context, the proposed expression for the critical stress is $\tau_c = \sqrt{\frac{\eta_\infty}{\lambda_s k_0}}$, where we find that the thixotropic inverse rate of energy-dissipation $\lambda_s \cdot k_0$ has an explicit impact on τ_c. A close inspection of τ_c-definition serves here to explain the influence of its components, where the second Newtonian-plateau η_∞-factor is modulated by the characteristic energy-dissipation rate $(\frac{1}{\lambda_s \cdot k_0})$ required for fluid-structure breakdown. Here, smaller $\lambda_s \cdot k_0$-products render larger energy dissipation rates required for structure fluidisation and, hence, larger critical stresses. Applying this reasoning to samples Healthy-1 and COPD-1, τ_c

appears higher for COPD-1 and indicates a larger critical stress: this difference ranges from $\tau_c = 0.18$ Pa for Healthy-1, to $\tau_c = 0.28$ Pa for COPD-1, which appear in quantitative agreement with the findings of Jory et al.[20], who determined critical-stress values ranging from 0.2 to 0.5 Pa, and other reports in the literature.[41]

In Fig.2, the response provided by the BMP+_τ_p model in oscillatory shear appears consistent with the experiments reported by Jory et al.[20]. Here, a frequency sweep at fixed deformation amplitude of $\gamma = 0.01$ illustrated in Fig.2a, renders $G' > G''$ in the frequency range below $\omega = 100$ rad/s, exhibiting the behaviour of an *elastic gel*. Beyond this frequency, the order swaps and G'' leads the rheological response. The model predictions describe quantitatively both moduli for frequencies below 10-20 rad/s for G', and around 50 rad/s for G'', with $R^2 \geq 0.90$. At higher frequencies, moduli are under-predicted. Nevertheless, the BMP+_τ_p follows the same trends observed experimentally. Furthermore, in Fig. 2b under a amplitude sweep at the fixed frequency of $\omega = 6.28$ rad/s, the BMP+_τ_p constitutive equation describes qualitatively the plateaued responses of G' and G'' up to a deformation of $\gamma = 0.1$ units, with quantitative accuracy only for sample Healthy-1; from this point, predictions depart from experiments. The beginning of the strain-thinning response for experimental data is observed around $\gamma = 0.1$, followed by a crossing point between G' and G'' at $\gamma = 1$, marking what experimentalist refer to as the *yield point*[20,71], falling in the category of a purely strain-thinning behaviour[62,70]. Meanwhile, the theoretical curves display thickening, besides an over prediction of G', which results in the estimation of a higher yield point, and in a different type of viscoelastic response: weak-strain overshoot[62,70]. Notwithstanding this contrast between the BMP+_τ_p description and the samples behaviour, the weak-strain overshoot viscoelastic response is seen in homologous systems, such as synthetic mucus samples under oscillatory shear, as reported by Lafforgue et al.[80] (see Fig. 3 therein), and yield-stress fluids, like Xanthan gum solutions (see Fig. 7b in Hyun et al.[70]). In Fig. 2, vertical-grey dashed lines signal the $\gamma\omega$-value of 0.1 s^{-1} below which the model applies for these specific tests. One should note that the $\gamma\omega$-span studied by Jory et al.[20] is notably large with respect to other studies, as will be evident in the distinct cases below. The BMP+_τ_p model is capable of predicting strain-thinning viscoelastic responses under relatively small λ_1-values (see more details in the Appendix); such circumstances are characteristic of weakly viscoelastic materials, regime outside the commonplace sputum rheology reported[5,11,17,19,20], for which the viscoelastic relaxation time ranges from some tenths to hundreds of units (see Tables 5-8). This explains why, even if we achieve a quantitative agreement in fitting steady shear flow curves and other experimental data sets, as we demonstrate in the following sections, there is room for improvement in describing LAOS data. This same position will be observed for all samples having amplitude-sweeps. We are performing studies on the predictive capabilities of the BMP+_τ_p model at the moment to extend the $\gamma\omega$-window and to capture the diversity of viscoelastic responses reported elsewhere[62,70], which will appear subsequently.

In Fig. 3, we compare the BMP+_τ_p modelling results for the Lissajous curves obtained under oscillatory deformations. It is worth mentioning that this type of plots highlight features that are not apparent in steady protocols or average viscoelastic material functions (G' and G''). Here, to achieve a satisfactory description of the Lissajous curves for the sample COPD-1 in Fig. 3, we considered an extra source of non-linearity in the form of a shear-banding mechanism, which provides additional shear-thinning features in the rheological response[58]. This shear-banding inclusion is in agreement with the characterisation reported by Jory et al.[20], where they

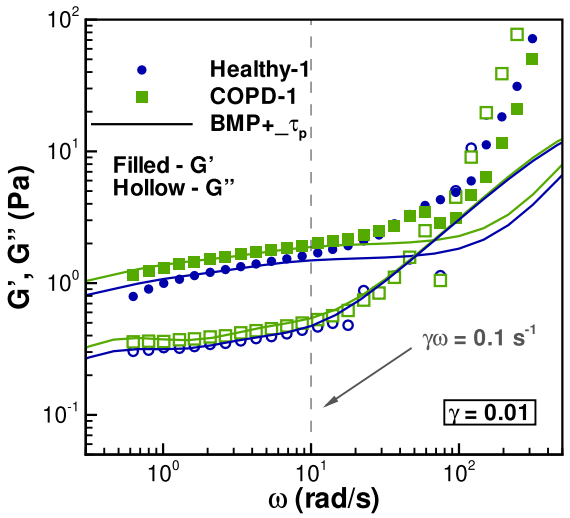

(a) Model predictions versus experimental data for samples Healthy-1 and COPD-1 in a frequency sweep. R^2(Healthy-1)= 0.90, R^2(COPD-1)= 0.92.

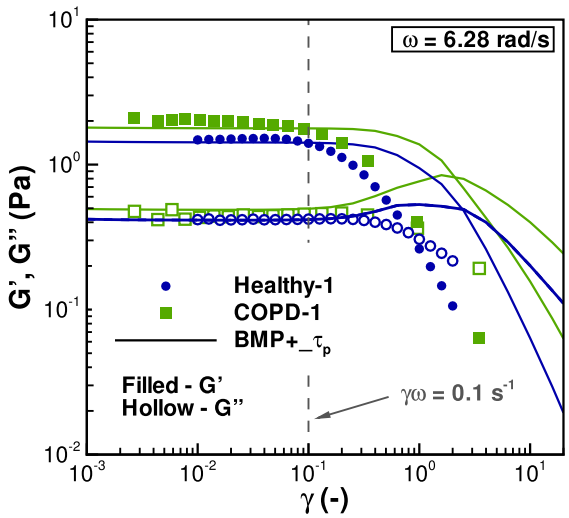

(b) Model predictions versus experimental data for samples Healthy-1 and COPD-1 in a strain sweep. R^2(Healthy-1)= 0.97, R^2(COPD-1)= 0.61.

Fig. 2. BMP+_τ_p-model predictions in oscillatory shear. Experimental data by Jory et al.[20]. In these figures, a measure of the shear rate for the experiment-to-model-prediction departure is provided under a vertical dashed-grey line signalling the $\gamma\omega = 0.1$ level for non-linear response; here, one should consider the frequency ω in Hz to maintain unit consistency.

used the Power-Law constitutive equation to characterise their sputum rheology data under negative Power-Law indexes to fit their data; these same findings are particular of shear-banding systems[58]. As reported in Table 5, the shear-banding intensity-parameter ν was considered only on the first stress mode, but its effects extend to large amplitudes of deformation. In line with the findings in Fig. 2, these elastic projections show agreement for relatively smaller amplitudes, for which the elliptical curves manifested by experiments are captured by the model. In contrast, for larger amplitudes, a stronger squared response is predicted, linked with the over-prediction of the plastic features of the sample. Nevertheless, it stands out that the shear-stress magnitudes are well-predicted with the BMP+_τ_p equation, allowing for a $R^2 \geq 0.88$.

The *extensional response of human mucus and sputum* is very scarcely treated in the literature[18], basically because its measurement is not easily attainable with commercial rheometers. Nevertheless, its importance has been recognised recently[18], since the deformation dominating sputum expectoration process is of mixed shear-to-extensional nature. As such, exploration of the extensional response of mucus and sputum is performed here from a theoretical perspective, via prediction of the extensional viscosity coefficient (η_E) in steady state (see Fig.1), and the tensile-stress growth coefficient (η_E^+) (Fig. 4), which are the basic material functions defined for transient uniaxial extension.

In Fig.1, the steady uniaxial extensional viscosity trends predicted by the BMP+_τ_p equation, using the parameter-set in Table 5, follow a strain-softening response: η_E decreases with extension rate $\dot{\epsilon}$-rise; here, predictions based on COPD-1 parameters display a notably larger extensional viscosity than the Healthy-1 case. It is noteworthy that this is a rather simple response in extension; as it will be shown latter, for the case of severe CF case, a complex strain-hardening and softening behaviour is reported - see on for further details.

In contrast, under transient uniaxial extension, highly non-linear trends are recorded from BMP+_τ_p -model predictions. In Fig.4, we chose to present the results in a dimensionless fashion, in order to make a fair comparison between results for samples Healthy-1 and COPD-1. Also, the span of selected Weissenberg numbers ($Wi = \lambda_1 \dot{\epsilon}_0$) lie on the non-linear regime, i.e., in the strain-thinning zone. As it is apparent in this figure, both Healthy-1 and COPD-1 concur with the linear viscoelastic (LVE) limit, given at relatively small times and at low *Wi* numbers, which satisfies $\eta_E^+(\dot{\epsilon}, t) = 3\eta^+(t)$. At $Wi = 100$, we observe a monotonic response, produced by a competition between viscoelastic relaxation mechanisms that originates from having different relaxation times (a λ_1-spectra) and their contrasting magnitudes. Departure from this relatively-simple behaviour happens at smaller times with larger *Wi*, and it is characterised by multiple overshoots, being way more pronounced in the Healthy-1 case. Predictions of multiple overshoots are also reported in the work of Lele & Mashelkar[81], and Islam[82]: the former study described the shear-induced transient rate-of-formation of hydrogen bonds in solutions of polar polymers, with the Energetically Crosslinked Transient Network (ECTN) model. The ECTN equation predicted more than one overshoot in the stress-growth coefficient (η^+)[81]; the latter study employed a variant of the Islam and Archer (IA) equation to model the response of polydisperse, linear polymers melts and solutions. Analogously, these authors observed two stress overshoots in the start-up plots of η^+, that were attributed to the contribution of different components, each one with widely-separated molar masses and relaxation times[82]. A similar plateaued response appeared also in the work of Varchanis et

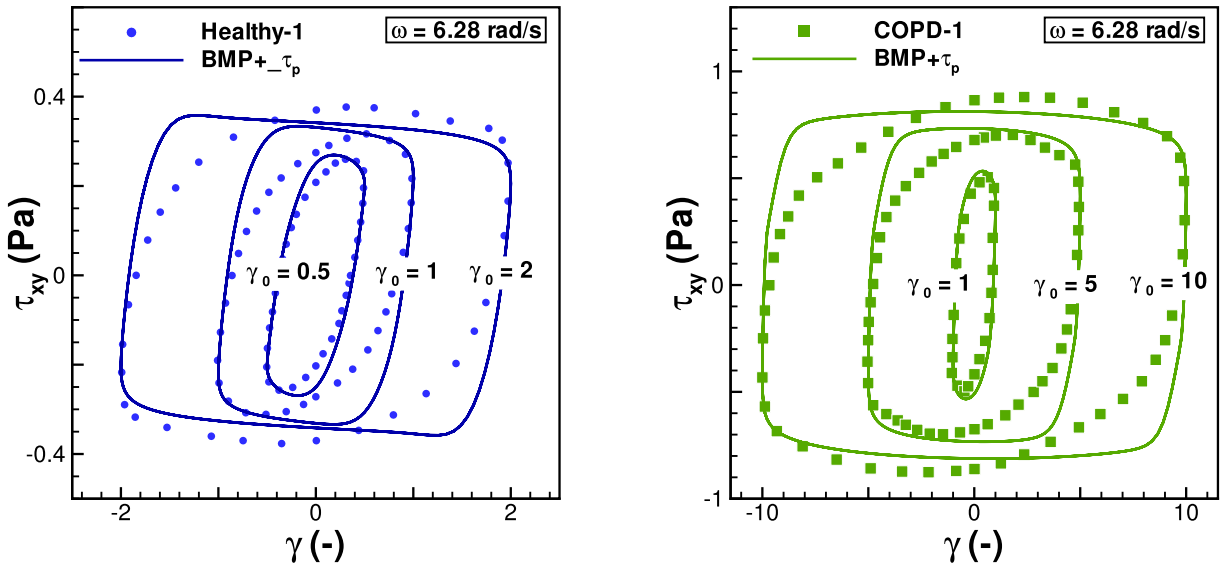

(a) Healthy-1 data against BMP+_τ_p-model predictions for $\gamma_0 = \{0.5, 1, 2\}$ units. $R^2 = \{0.98, 0.88, 0.92\}$ respectively.

(b) COPD-1 data against BMP+_τ_p-model predictions for $\gamma_0 = \{1, 5, 10\}$ units. $R^2 = \{0.98, 0.95, 0.90\}$ respectively.

Fig. 3. BMP+_τ_p-model predictions in oscillatory shear for samples Healthy-1 and COPD-1 at fixed $\omega = 6.28$ rad/s. Elastic Lissajous projections. Note the difference in plot scale across cases, marking different levels in the magnitude of shear stress τ_{xy} and deformations γ applied. Symbols: Experimental data by Jory et al.[20].

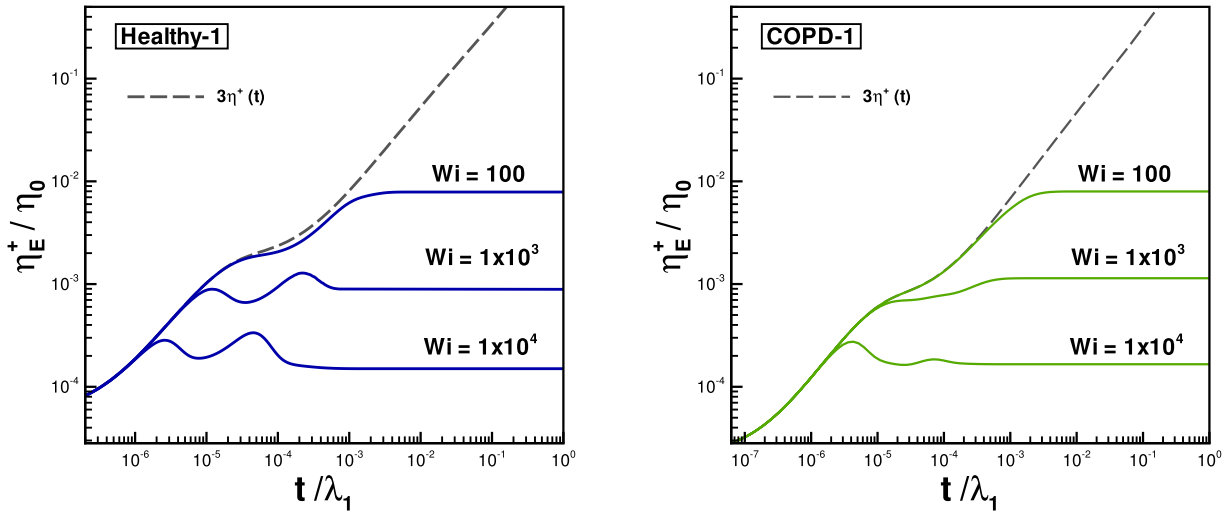

(a) Healthy-1 transient uniaxial extensional growth coefficient η_E^+ for $Wi = \{10^2, 10^3, 10^4\}$ units.

(b) COPD-1 transient uniaxial extensional growth coefficient η_E^+ for $Wi = \{10^2, 10^3, 10^4\}$ units.

Fig. 4. BMP+_τ_p-model predictions for unsteady extensional flow (uniaxial elongation) for samples Healthy-1 and COPD-1. Dimensionless extension-rate measure: $Wi = \lambda_1 \dot{\epsilon}$.

al.[83], where the authors described the behaviour of a TVEP material in step-up shear with the model Saramito/Herschel Bulkley-Isotropic-Kinematic-Hardening (SHB-IKH).

Contrasting healthy, COPD and CF samples through rheological characterisation (Healthy-2, CF-2 and COPD-2 from Patarin et al.[19])

In this section, the rheological characterisation of the experimental data reported by Patarin et al.[19] with the BMP+_τ_p model is presented in terms of the comparison between control sample Healthy-2 data-set against ill-conditioned samples COPD-2 and CF-2. The objective of this section is to give evidence of the distinct rheological responses across COPD and CF affecting human sputum. One should note that the rheological protocols followed by Patarin et al.[19] are not as exhaustive as those by Jory et al.[20] (see Table 3); Patarin et al.[19] only provide frequency and amplitude sweeps, over which we perform our theoretical rheological characterisation. Once a BMP+_τ_p parameter-set is determined, we provide predictions in steady simple shear, uniaxial extensional flow, and LAOS.

In Fig.5, we compare the experimental response of samples Healthy-2, COPD-2 and CF-2 against the model fitting results, under the parameter-sets listed in Table 6. Overall, the BMP+_τ_p description of the experimental G' and G'' moduli coincide qualitatively with the mechanical response of Patarin et al.[19] sputum samples. The best quantitative agreement is achieved for frequency sweeps ($R^2 \geq 0.83$), and like in the previous cases, the accuracy is reduced in amplitude sweeps ($R^2 \geq 0.6$). As expected, we see a viscoelastic gel-like response with G' dominating the SAOS window-of-observation at relatively small frequencies and deformation amplitudes. In contrast to previous findings for the data-set from Jory et al.[20], the viscoelastic time scale λ_1 for sample Healthy-2 is significantly larger ($\lambda_1 = 600$ s), even compared to λ_1-values for samples COPD-2 ($\lambda_1 = 180$ s) and CF-2 ($\lambda_1 = 410$ s). This indicates that even for sputum samples sharing the same *consistency* (as for Healthy-1 and Healthy-2), they may display totally different transient responses, impacting the transport processes in physiological systems. It is noteworthy how the moduli response segregate across samples Healthy-2, COPD-2 and CF-2, for which Healthy-2 displays the weaker G' and G'' response, followed by COPD-2 and surpassed by CF-2. Such differences in moduli magnitude may rely in the illness severity (as it is demonstrated later in this work), and the trends found within this theoretical characterisation may not be representative of all COPD and CF severity degrees, but rather of specific case-studies. Then, the experimental data fitted in Fig. 5 reveal that the magnitude of G' and G'' on their own may not be a suitable way to distinguish one illness from another across isolated studies and would require complementary rheological tests, such as thixotropic tests to reveal other time-dependent responses. Nevertheless, G' and G'' signals may be sufficient to identify the effects of an obstructive disease in isolated cases[19], and can provide valuable information on its severity and treatment progress.

Predictions of shear and extensional viscosity are displayed in Fig. 6. There is a drop of four-to-five orders-of-magnitude in both η and η_E between the first and the second Newtonian plateau levels (see Table 6), finding the largest gap for sample CF-2. In the case of η_E, we identify that all samples show a purely strain-softening response. As stated before, the product of the thixotropic parameters $\lambda_s \cdot k_0$ determines the strength of the thinning response and τ_c, which is connected to the plastic features of sputum. Concerning the values of τ_c reported in Table 6, we observe that the critical stress amounts $\tau_c = 0.07$ Pa for sample Healthy-2, whilst for samples COPD-2 and CF-2, τ_c grows one and two orders-of-magnitude, respectively: $\tau_c = 0.63$ Pa for sample COPD-2 and $\tau_c = 1.29$ Pa for CF-2. This relationship between τ_c and $\lambda_s \cdot k_0$ marks a distinctive trend between

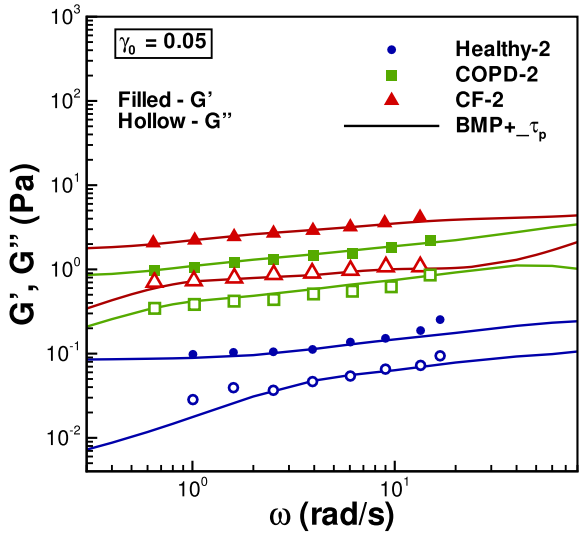

(a) Comparison between samples Healthy-2, COPD-2 and CF-2 in a frequency sweep. $R^2 = \{0.83, 0.88, 0.94\}$ respectively.

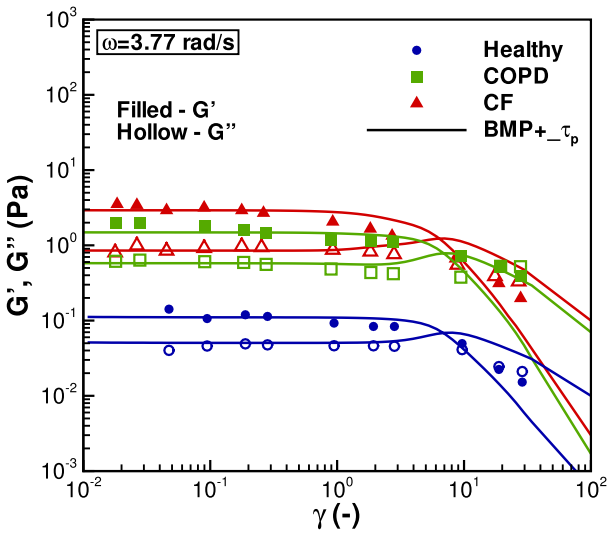

(b) Comparison between samples Healthy-2, COPD-2 and CF-2 in a strain sweep. $R^2 = \{0.84, 0.60, 0.83\}$ respectively.

Fig. 5. BMP+_τ_p-model predictions in oscillatory shear. See BMP+_τ_p parameter-sets in Table 6. Symbols: experimental data from Patarin et al.[19].

Parameter	Mode 1	Mode 2	Mode 3	Mode 4
Healthy-2				
η_{p_0} (Pa.s)	50.0	$1.3x10^{-2}$	0.01	$4.0x10^{-3}$
η_∞ (Pa.s)	$1.0x10^{-4}$	$1.0x10^{-4}$	$1.0x10^{-4}$	$1.0x10^{-4}$
$\lambda_1(s)$	600.0	0.20	3.0	$1.0x10^{-3}$
$\lambda_s * k_0$ (Pa^{-1}s)	0.02	0.01	1.0	1.0
τ_c (Pa)	**0.07**	0.10	0.01	0.01
COPD-2				
η_{p_0} (Pa.s)	145.0	0.55	0.10	0.04
η_∞ (Pa.s)	$1.0x10^{-4}$	$1.0x10^{-4}$	$1.0x10^{-4}$	$1.0x10^{-4}$
$\lambda_1(s)$	180.0	1.0	0.16	0.03
$\lambda_s * k_0$ (Pa^{-1}s)	$2.5x10^{-4}$	$5.0x10^{-4}$	0.01	0.01
τ_c (Pa)	**0.63**	0.45	0.10	0.10
CF-2				
η_{p_0} (Pa.s)	700.0	1.0	0.14	$2.5x10^{-2}$
η_∞ (Pa.s)	$1.0x10^{-4}$	$1.0x10^{-4}$	$1.0x10^{-4}$	$1.0x10^{-4}$
$\lambda_1(s)$	410.0	0.90	0.11	$5.0x10^{-3}$
$\lambda_s * k_0$ (Pa^{-1}s)	$6.0x10^{-5}$	$1.0x10^{-3}$	0.01	0.01
τ_c (Pa)	**1.29**	0.32	0.10	0.10

Table 6. Fitting parameters for samples Healthy-2, COPD-2 and CF-2.

the rheological response of sputum across illnesses, and provides evidence of the link between the plastic nature of sputum with its thixotropic features, captured theoretically with the BMP+_τ_p model for the first time in sputum and mucus rheological studies - at least, to the best of the our knowledge. This link between plasticity and thixotropy is a current topic in the field of theoretical modelling of complex materials[73]. These results indicate that rather than focusing only on the *consistency of sputum*, one should pay attention as well on the comparison between rheological timescales, where the viscoelastic and thixotropic characteristics reside.

The BMP+_τ_p-model predictions under transient uniaxial extension are provided in Fig. 7. As expected from the steady results in Fig. 6, sample CF-2 displays the largest η_E^+ compared to samples Healthy-2 and COPD-2. A detailed inspection of the CF-2 gives evidence of weak overshoots occurring in the range $10^{-4} < \dot{\epsilon} < 10^{-3} s^{-1}$,

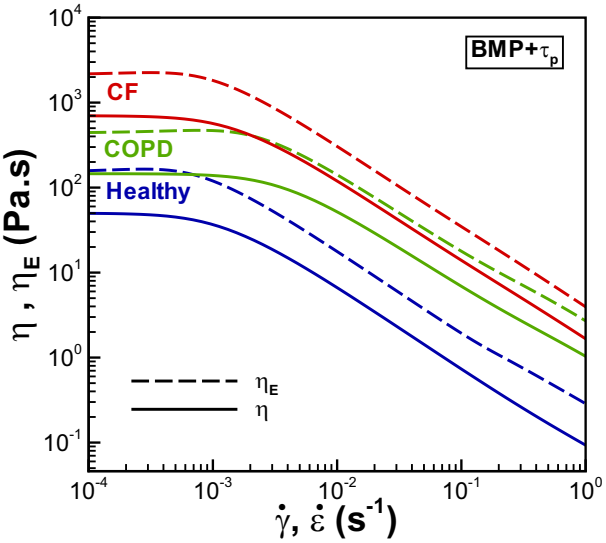

Fig. 6. BMP+_τ_p-model predictions in simple shear and uniaxial elongation for samples Healthy-2, COPD-2 and CF-2. See parameters in Table 6.

which is qualitatively different from the other samples. In contrast to Fig 4, the predicted transient extensional response in Fig.7 for these cases appears rather simpler, possibly due to the experimental protocol used by Patarin et al.[19], which hindered the determination of characteristic timescales), for which no transient test were performed, contrary to the characterisation protocol followed by Jory et al.[20]

Figures 8 and 9 illustrate the Lissajous elastic projections of samples and model description in oscillatory shear under the parameter sets in Table 6. We selected a frequency and amplitude span where the BMP+_τ_p predictions were validated, according the fitting in Fig. 5: $\omega = [1, 10]$ rad/s, and $\gamma_0 = [0.1, 10]$, respectively. This range of deformation conditions hinders the appearance of a predominantly viscoelastoplastic regime on the Pipkin diagrams, as we cannot see the theoretical limit of a collapsed diagonal (marking a purely elastic response), nor a full circle (marking a purely viscous response in elastic projections[63]). Instead, one observes a variety of non-Newtonian signatures, that are qualitatively similar from case to case. At relatively small frequencies, and from small to moderate amplitudes (at least, moderate enough so the curves do not present sudden increments in stress), Lissajous curves display the typical trajectory of a post-yielded visco-plastic system[84]. At larger amplitudes, we observe sudden increments on the shear stress, that appear as over and undershoots. This signals the transition to a highly non-linear thixo-viscoelastoplastic regime[85], where the time-dependent (although not necessarily transient) response, e.g. the stress-relaxation mechanism, is dominated not only by the λ_1-spectra, but also by the λ_s thixotropic timescales. At higher frequencies, the yielding occurs at even smaller amplitudes and the viscous contributions become relevant, since the curves acquire a rather elliptical shape, even though the frequency sweep in Fig. 5 demonstrates that $G' > G''$ along the studied ω-span. Then, through the BMP+_τ_p-model description, in contrast with the common-place consideration of sputum being an elasto-viscous solid, we infer that there exist some instances where its *fluidisation* cannot be determined by the $G' = G''$ intersection point in amplitude sweeps, as this transition depends on both γ and ω. This is not surprising, considering that the yield point for thixotropic gels, such as sputum, is recognised to deviate from the expected responses of viscoelastoplastic materials in oscillatory shear[71]. Therefore, average material functions such as moduli condensate the general characteristics of the rheological behaviour of sputum, but the richness of its response deserves to be explored through dynamic, non-linear experimental and theoretical frameworks, such as LAOS and its representation in Pipkin diagrams, as the ones in Figs. 8 and 9, since they may reveal features that may be disease-dependent, as theoretically predicted in this work.

Also, in Figs. 8 and 9, we give explicit evidence of the relatively-stronger plastic features of samples COPD-2 and CF-2 via predictions with the BMP+_τ_p model, in connection with what happens physiologically with sputum in the airways, where the plastic features of the material rule its behaviour, blocking the airways[18,47,67,68]. Particularly in the regime of relatively small frequencies and large deformations, one may note the marked squared loops, which are a common signature for yield-stress fluids, as apparent in Fig.8 for the Healthy-2 case. Comparatively, in Fig.9, the CF-2 case displays markedly-squared with respect to sample Healthy-2 and COPD-2. As such, this kind of data in the form of a Pipkin diagram reveals distinctive behaviour across illnesses and may serve as a qualitative reference to determine the illness severity in affected patients, with the potential of serving as a tool to test and measure the effectiveness of mucolytic treatments, which have the main aim of restoring in some extent the consistency of healthy mucus and sputum to enhance the expectoration process[11].

In a closer inspection of these highly-non-linear responses, the transition from a viscoelastoplastic to a thixo-viscoelastoplastic regime shown in Figs. 8 and 9, is evidenced in Fig. 10, where the viscous Lissajous projections (Figs. 10d, 10e and 10f) show that at larger amplitudes, secondary loops appear (given by the self-intersection of curves). According to Ewoldt & McKinley[85], secondary loops occur when the thixotropic re-structuration

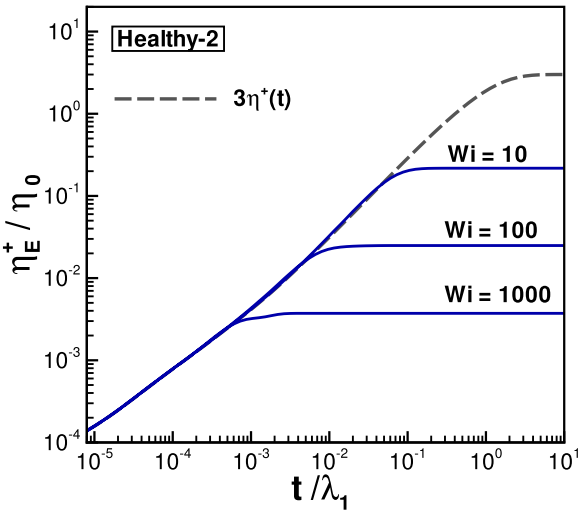

(a) Healthy-2 transient uniaxial extensional growth coefficient η_E^+ for $Wi = \{10, 10^2, 10^3\}$ units.

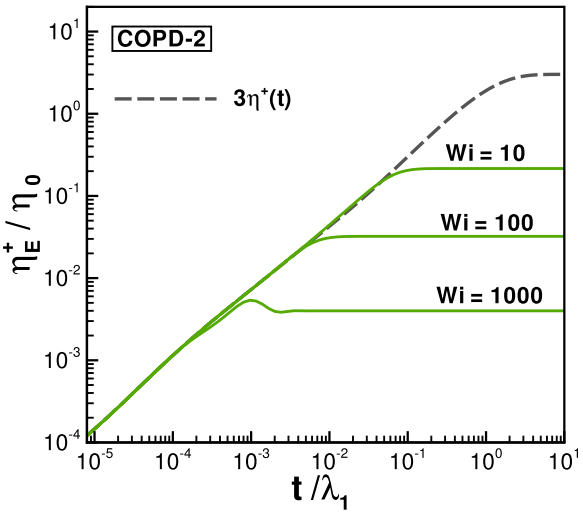

(b) COPD-2 transient uniaxial extensional growth coefficient η_E^+ for $Wi = \{10, 10^2, 10^3\}$ units.

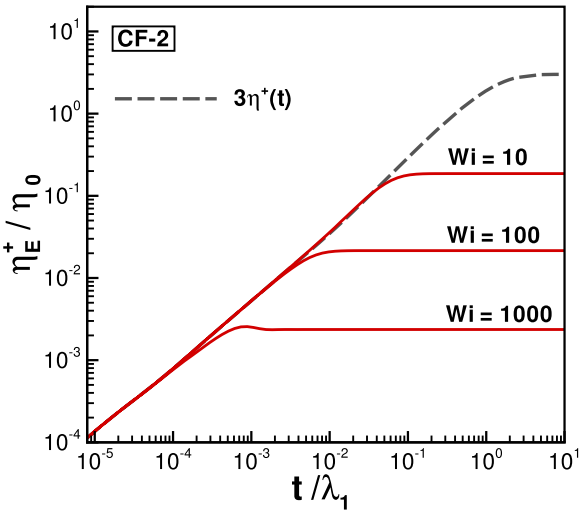

(c) CF-2 transient uniaxial extensional growth coefficient η_E^+ for $Wi = \{10, 10^2, 10^3\}$ units.

Fig. 7. BMP+_τ_p-model predictions for unsteady extensional flow (uniaxial elongation) for samples Healthy-2, COPD-2 and CF-2. Dimensionless extension-rate measure: $Wi = \lambda_1 \dot{\epsilon}$.

timescale is smaller than the oscillatory deformation timescale, then allowing for microstructure build-up, or as a result of strong elastic non-linearity. Then, this predictions are susceptible to the choice on λ_s and k_0 model parameters for each mode, whose determination requires a thorough rheological characterisation of the samples under exhaustive transient protocols. Unfortunately, the experimental data set of Patarin et al.[19] did not include rheometric tests from where to obtain this specific information, e.g, hysteresis loops. Nevertheless, the BMP+_τ_p model is able to predict such transition signatures, giving further information on the thixo-viscoelastoplastic, gel-like nature of human sputum. Moreover, these kind of differentiated prediction may be an additional ingredient to a computationally-driven characterisation protocol of human mucus-sputum, from which distinct disease-conditioned behaviour may be captured and categorised through advanced rheological tests.

Contrasting CF samples through rheological characterisation (samples CF-3, CF-4, CF-5 from Nielsen et al.[11], Dawson et al.[5], and Tomaiuolo et al.[17])

In this section, we provide evidence of the BMP+_τ_p theoretical characterisation of the experimental results reported by Nielsen et al.[11], Dawson et al.[5], and Tomaiuolo et al.[17], reflecting the influence of CF in human sputum, for which we contrast cases with different illness severity and its rheological manifestation.

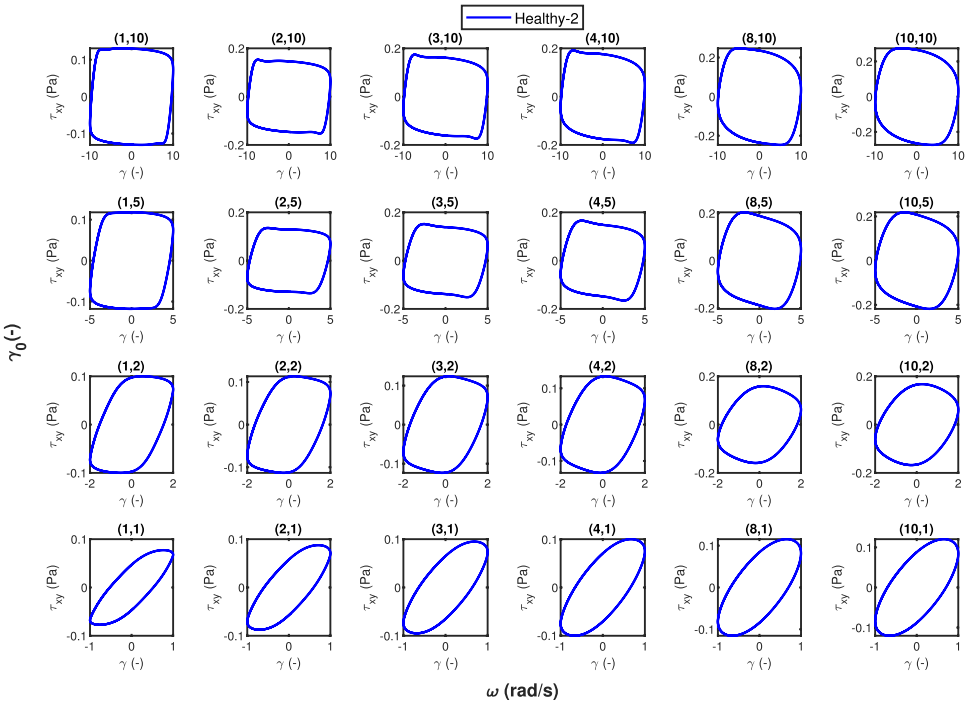

Fig. 8. BMP+_τ_p-model predictions in oscillatory shear for sample Healthy-2. Elastic Lissajous projections.

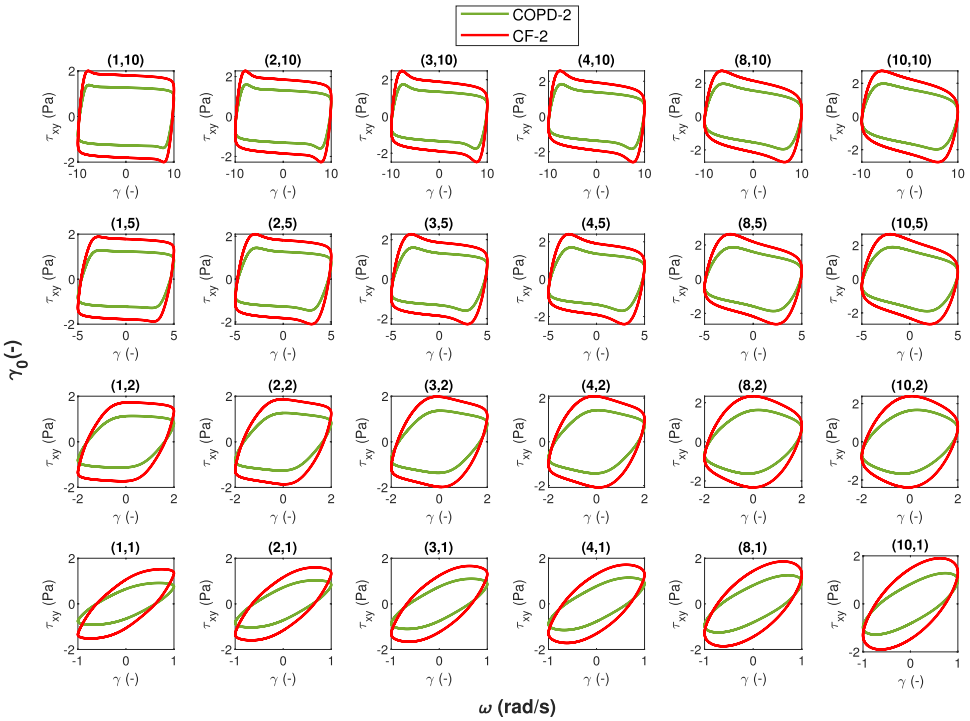

Fig. 9. BMP+_τ_p-model predictions in oscillatory shear for samples COPD-2 and CF-2. Elastic Lissajous projections.

Starting with the comparison between samples CF-3 and CF-4, we observe quantitative agreement between experimental data[5,11] and the BMP+_τ_p predictions in Figs.11 and 12 (with $R^2 \geq 0.81$, except for the amplitude sweep of CF-4). Listed in Table 7, we provide the model fitting parameters for samples CF-3 and CF-4. In addition to the main features identified in the rheological response of sample CF-2, which also appear in the case of CF-3 (i.e., a pronounced shear and strain thinning behaviour, and gel-like response in oscillatory shear),

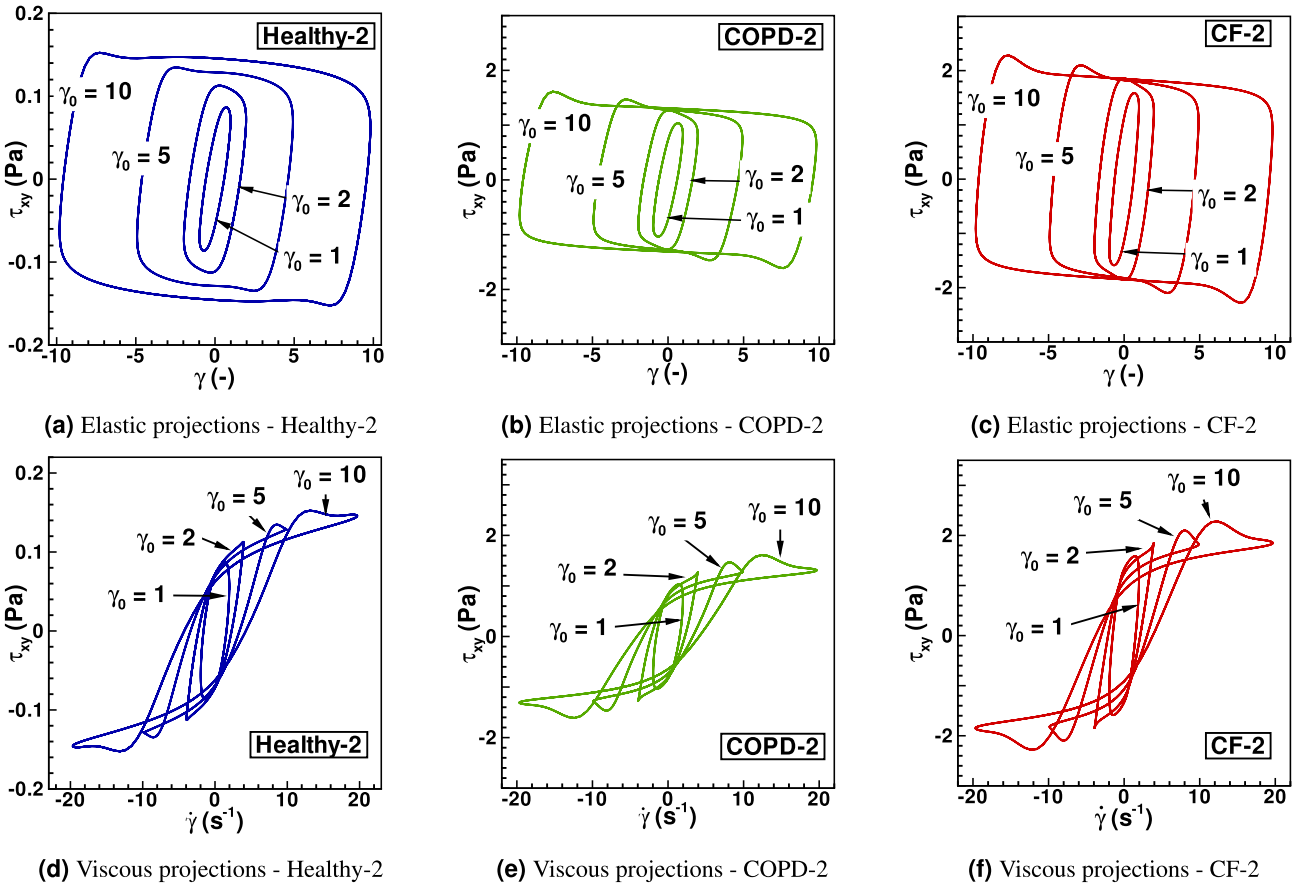

(a) Elastic projections - Healthy-2 **(b)** Elastic projections - COPD-2 **(c)** Elastic projections - CF-2

(d) Viscous projections - Healthy-2 **(e)** Viscous projections - COPD-2 **(f)** Viscous projections - CF-2

Fig. 10. Extract from the Pipkin diagrams in Fig. 8 and 9, $\omega = 2$ rad/s. Note the different scale in the shear stress needed to report Healthy-2 predictions in contrast with COPD-2 and CF-2, for which the ill-conditioned samples display shear-stress signals one order-of-magnitude larger than those under the healthy sample.

the hysteresis loop in Fig. 11b accounts for the strong thixotropic response of CF-sputum. This specific piece of information allowed us to determine the value of $\lambda_s = 50$ s. The comparison of $\lambda_s = 50$ s and $\lambda_1 = 250$ s is in-line with general biogel characteristics, as reported by Ewoldt and McKinley[86], where, for such kind of materials, the viscoelastic characteristic time λ_1 is significantly larger than the re-structuration time λ_s.

The rheometric-data and theoretical-prediction trends displayed in Fig. 12 for sample CF-4 are quite similar to those of CF-3 in Fig. 11, except for the behaviour of η_E^+ (see Fig.12c): here, η_E^+ displays a marked strain hardening-to-softening response, with a η_E-maximum registered at around $10^{-2}\ s^{-1}$, followed by a steep drop of the extensional viscosity with extension-rate rise. This hardening around the transition from the linear to the non-linear regime, of which there would be no indication if the analysis of the response in uniaxial extensional flow were left out, appears also in further exploration of the BMP+_τ_p model predictions for CF-affected sputum from the work of Tomaiuolo et al.[17], in which samples of mild, moderate and severe CF sputum are characterised.

The BMP+_τ_p-model fittings and tabulated parameter-sets (see Table 8), for the data sets found in the work of Tomaiuolo et al.[17], are based on the available steady simple shear apparent viscosity data and SAOS protocols, for which qualitative agreement is attained, but the quantitative description appears reduced by the out-of-tendency experimental points (if compared with the tendency followed by CF-2 to CF-4). First of all, the usual viscosity drop is captured under a span of some six orders-of-magnitude according with the relative level from the first (η_{p0}) to the second Newtonian plateaux (η_∞), being the severe CF case the one with the largest apparent viscosity. In line with these trends, the severe CF-case holds the largest viscoelastic relaxation time $\lambda_1 = 250$ s and the largest critical stress for $\tau_c = 10$ Pa.

Worthy of note are the extensional viscosity η_E-trends in Fig.13 extracted from predictions under the BMP+_τ_p-model formalism and its corresponding parameters-sets in Table 8. Here, the strain hardening-to-softening features of these CF-5 sputum samples correlates with the severity of illness. Reportedly, the CF-5 mild case displays a relatively mild strain-hardening rising trend at intermediate extension-rates in the range $10^{-2} < \dot{\epsilon} < 10^{-1}\ s^{-1}$, in contrast to the clinically-qualified as very-severe case, that displays a prominent η_E-peak rising over an order-of-magnitude from the Newtonian plateau at vanishing extension-rates, even appearing sooner in the extension-rate range of $10^{-3} < \dot{\epsilon} < 10^{-1}\ s^{-2}$. Recall that the strength of extensional-hardening correlates directly with the magnitude of the BMP+_τ_p thixotropic rate of energy dissipation ($\frac{1}{\lambda_s \cdot k_0}$), making

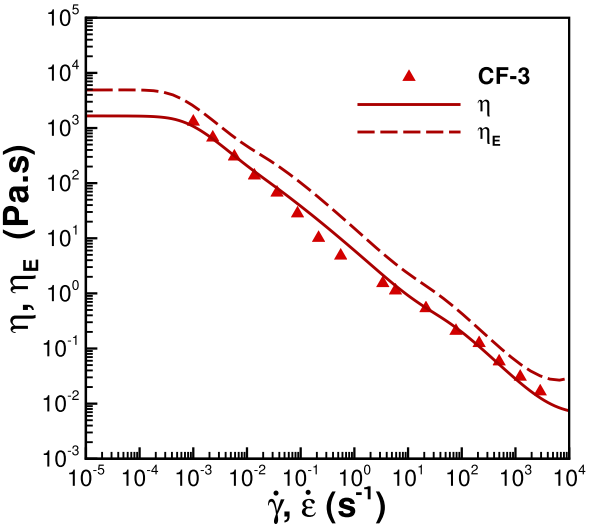

(a) BMP+_τ_p-model predictions in steady shear and uniaxial extension flows. $R^2 = 0.98$

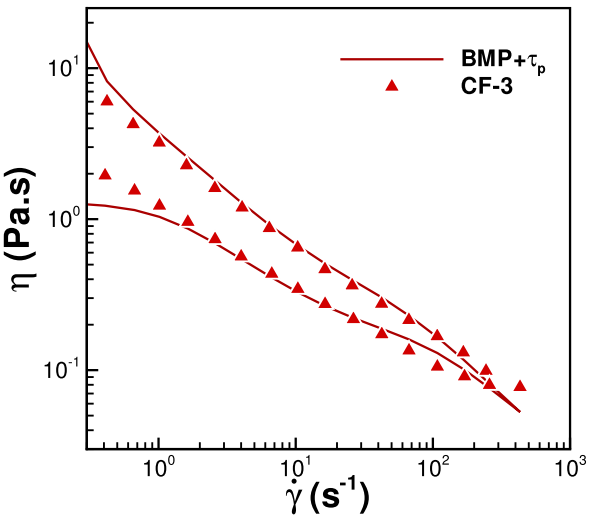

(b) BMP+_τ_p-model predictions for a hysteresis loop. $R^2 = 0.81$

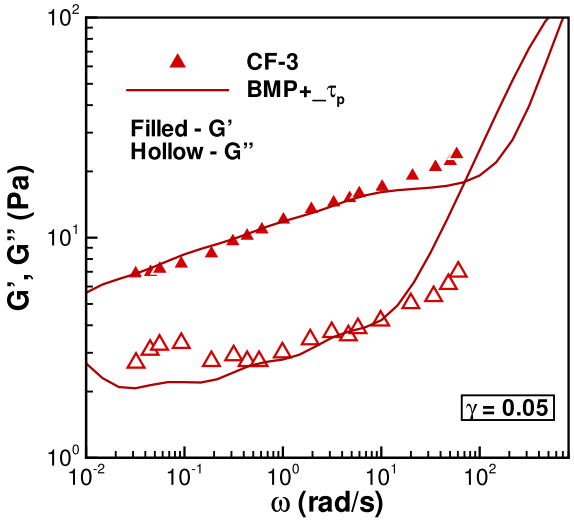

(c) BMP+_τ_p-model predictions in a frequency sweep in SAOS. $R^2 = 0.82$

Fig. 11. BMP+_τ_p-model predictions for sample CF-3. See parameters in Table 7. Symbols: Experimental data from Nielsen et al.[11].

this behaviour highly complex and related to a thixo-viscoelastoplastic response. In Table 8, the very-severe case holds the smallest $\lambda_s \cdot k_0$ product across cases in Tomaiuolo et al.[17], amounting $\lambda_s \cdot k_0 = 10^{-6}$ units, and translating into a characteristic thixotropic energy-dissipation rate of $(\frac{1}{\lambda_s \cdot k_0}) = 10^6\ Pa \cdot s$. Fig.14 displays the response of G' and G'' moduli, illustrating a direct correlation between CF-severity and moduli magnitude, with the severe case displaying the largest G' and G'' levels. Here, the BMP+_τ_p performance is consistent with the expected magnitude and trends. It is important to note that the richness of the present analysis is due to comparison between cases associated to a different illness-severity degree. Making this kind of contrast through rheological characterisation for other diseases, such as COPD, could point out the uniaxial-extension material functions and the determination of characteristic time scales as the basis to develop biomarkers for treatment monitoring, even respiratory disease diagnosis.

Complementarily, in Fig.15, the transient extensional-deformation response of CF-5 cases is illustrated. We observe a switch from the strain-softening behaviour of samples CF-3 and CF-4, to a strain-hardening transient response for CF-5 samples, as the CF-5 curves lie above the LVE curve. This feature is accentuated in the severe and very-severe cases. These findings are relevant, since the physiological rates of extension in the airways (specially in the lungs[42,87]) fall within the deformation range where this hardening takes place, i.e., creeping

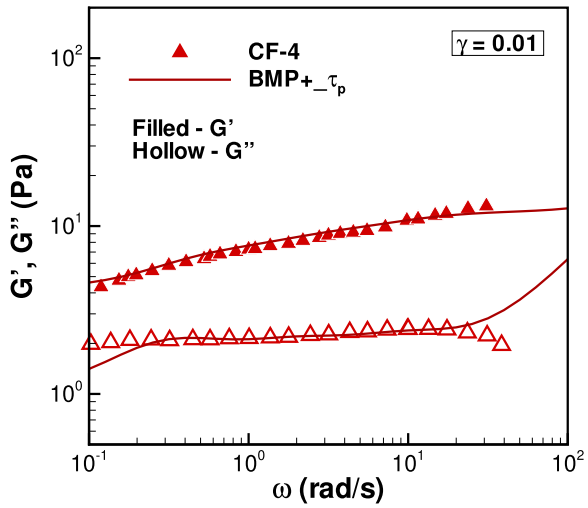

(a) BMP+_τ_p-model predictions in a frequency sweep in SAOS. $R^2 = 0.96$

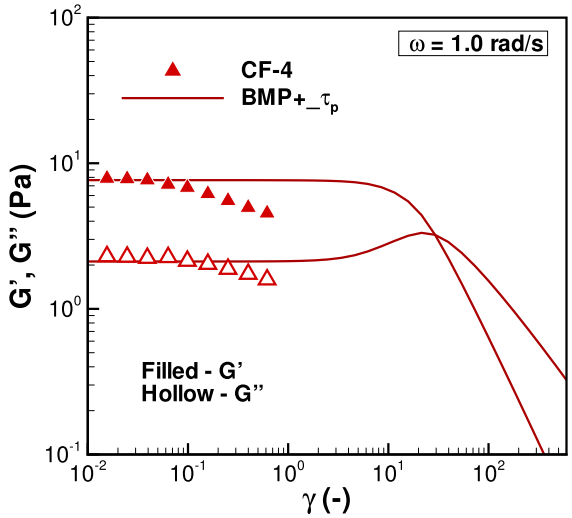

(b) BMP+_τ_p-model predictions in a strain sweep in SAOS. In this case, no quantitative agreement was achieved

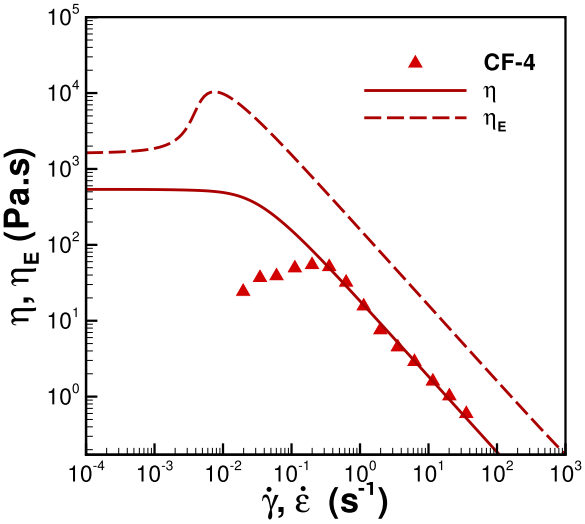

(c) BMP+_τ_p-model predictions in steady shear and uniaxial extension flows. $R^2 = 0.94$ (considering data at $\dot{\gamma} > 0.05$)

Fig. 12. BMP+_τ_p-model predictions for sample CF-4. See parameters in Table 7. Symbols: Experimental data from Dawson et al.[5].

flow conditions, explaining somehow the hindered process of expectoration that CF patients experience and the worsening of such symptom, according to the illness severity, and considering that uniaxial extension is relevant in the complex mixed shear-to-extensional flow of sputum, e.g. during the closure and reopening of airways[45]. Moreover, this increase in extensional viscosity, which can be referred to as extension-hardening, is also observed in homologue systems, such as mucin solutions[65], and saliva [66]. Until this point, such phenomenon has been predicted only for CF-affected sputum samples, but further rheometric measurements are needed to discard its manifestation in the case of COPD mucus and sputum. If discarded, this would serve as the basis for a diagnose biomarker. In this sense, we hypothesise that the rheological response in uniaxial extension may help to generate a more robust biomarker for pulmonary obstructive-disease diagnosis, assuming that thorough rheological transient and steady rheometric tests should be performed on sputum samples with different degrees of illness-severity.

Conclusions

In this work, we have carried out a thorough rheological characterisation on several samples of human mucus and sputum affected by COPD and CF[5,11,17,19,20] using a model-variant in the BMP family of fluids; the BMP+_τ_p model in a multi-modal approach[56–58]. Such study involves the mathematical modelling of rheometric flows, such

Parameter	Mode 1	Mode 2	Mode 3	Mode 4	Mode 5
CF-3					
η_{p0} (Pa.s)	1610.0	40.0	6.0	1.1	0.25
η_{∞} (Pa.s)	$1.0x10^{-4}$	$1.0x10^{-4}$	$0.4x10^{-4}$	$0.4x10^{-4}$	$5.0x10^{-3}$
$\lambda_1(s)$	250.0	15.0	1.9	0.25	$1.0x10^{-3}$
$\lambda_s * k_0$ (Pa^{-1}s)	$3.5x10^{-5}$	$2.0x10^{-5}$	$1.5x10^{-5}$	$1.5x10^{-5}$	$1.5x10^{-5}$
λ_s (s)	50.0	10.0	5.0	1.0	1.5
λ_1/λ_s	5.0	1.5	0.4	0.3	$7x10^{-4}$
ν (s)	0.0	0.0	0.0	0.0	0.0
τ_c (Pa)	**1.69**	2.2	1.63	1.63	18.2
CF-4					
η_{p0} (Pa.s)	520.0	10.0	1.1	0.25	0.06
η_{∞} (Pa.s)	$1.0x10^{-4}$	$1.0x10^{-4}$	$1.0x10^{-4}$	$1.0x10^{-4}$	$1.0x10^{-4}$
$\lambda_1(s)$	120.0	3.2	0.5	0.1	$1.0x10^{-3}$
$\lambda_s * k_0$ (Pa^{-1}s)	$7.0x10^{-7}$	$5.0x10^{-6}$	$1.0x10^{-5}$	$1.0x10^{-5}$	$1.0x10^{-5}$
τ_c (Pa)	**12.0**	4.5	3.2	3.2	3.2

Table 7. Fitting parameters for CF-3 and CF-4 samples.

Parameter	Mode 1	Mode 2	Mode 3	Mode 4
Mild				
η_{p0} (Pa.s)	10.0	2.0	0.25	0.06
η_{∞} (Pa.s)	$1.0x10^{-4}$	$1.0x10^{-4}$	$1.0x10^{-3}$	$1.0x10^{-3}$
$\lambda_1(s)$	15.0	4.5	0.5	$1.0x10^{-3}$
$\lambda_s * k_0$ (Pa^{-1}s)	$1.0x10^{-4}$	$1.0x10^{-4}$	$1.0x10^{-3}$	$8.0x10^{-5}$
τ_c (Pa)	**1.0**	1.0	1.0	3.5
Severe				
η_{p0} (Pa.s)	40.0	1.4	0.25	0.05
η_{∞} (Pa.s)	$1.0x10^{-4}$	$1.0x10^{-4}$	$1.0x10^{-3}$	$1.0x10^{-3}$
$\lambda_1(s)$	25.0	1.8	0.25	$1.0x10^{-3}$
$\lambda_s * k_0$ (Pa^{-1}s)	$2.0x10^{-6}$	$1.0x10^{-5}$	$5.0x10^{-5}$	$5.0x10^{-6}$
τ_c (Pa)	**7.07**	3.16	4.47	14.14
Very severe				
η_{p0} (Pa.s)	300.0	3.5	0.4	0.1
η_{∞} (Pa.s)	$1.0x10^{-4}$	$1.0x10^{-4}$	$1.0x10^{-3}$	$1.0x10^{-3}$
$\lambda_1(s)$	250.0	3.5	0.4	$1.0x10^{-3}$
$\lambda_s * k_0$ (Pa^{-1}s)	$1.0x10^{-6}$	$8.0x10^{-6}$	$2.0x10^{-5}$	$2.0x10^{-5}$
τ_c (Pa)	**10.00**	3.53	7.07	7.07

Table 8. Fitting parameters for CF-5 sample.

as steady and transient simple shear, uniaxial extension and oscillatory small and large amplitude deformations, i.e., SAOS and LAOS, which reveal a rich rheological response in linear and non-linear regimes, unveiling the complex thixo-viscoelastoplastic nature of human mucus and sputum. The correlation of these non-Newtonian features with the BMP+_τ_p-model parameters, through the critical stress for yielding and the corresponding thixotropic construction-destruction parameters, provides valuable information on the extensional response of human mucus and sputum for physiological airway-clearance functions[18,44,45].

Novel to previous proposals[43,47], we obtained - by theoretical predictions- information about the extensional response of sputum in healthy and ill-states[18,44,45], finding a direct relationship between the BMP+_τ_p model thixotropic parameters and the degree of thickening of sputum under flow conditions relevant in physiological process. These pieces of information can be used on the simulation of physiological process, like the mucociliary clearance, and also as the basis to develop biomarkers to monitor the efficacy of treatments for obstructive pulmonary diseases.

We summarise our conclusions regarding the theoretical characterisation of mucus and sputum samples as follows:

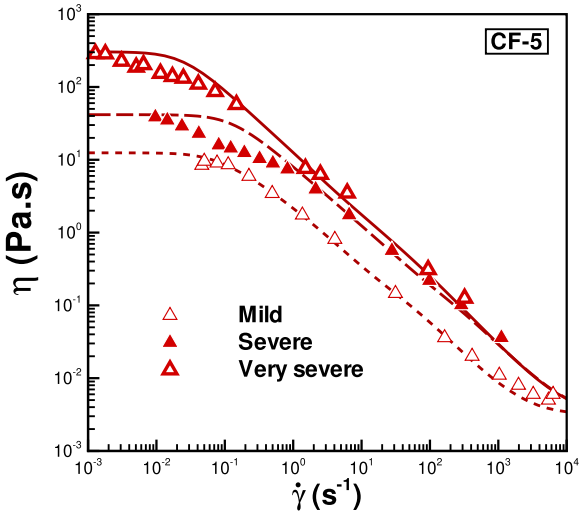

(a) BMP+_τ_p-model predictions in steady simple shear flow. $R^2 = \{0.97, 0.42, 0.57\}$ (Mild, Severe and Very severe.)

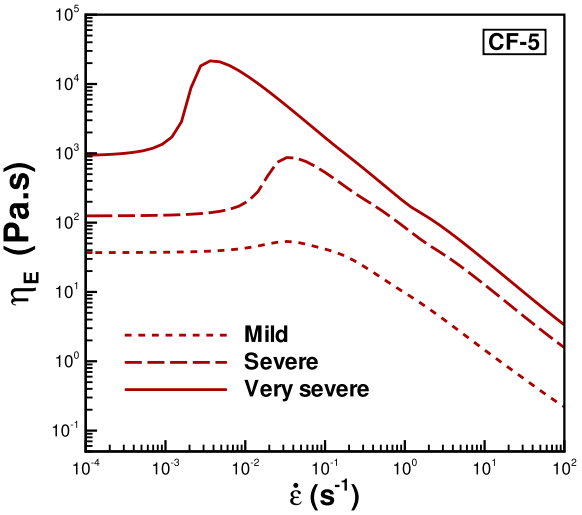

(b) BMP+_τ_p-model predictions in steady uniaxial extensional flow.

Fig. 13. BMP+_τ_p-model predictions for CF-5 samples. See parameters in Table 8. Symbols: Experimental data from Tomaiuolo et al.[17].

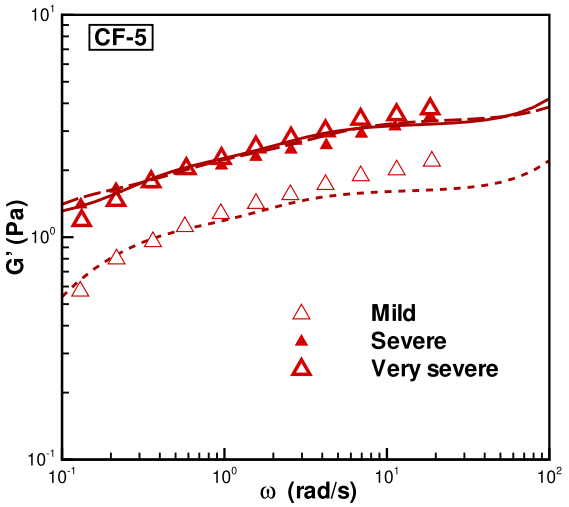

(a) BMP+_τ_p-model storage modulus G' predictions in SAOS.

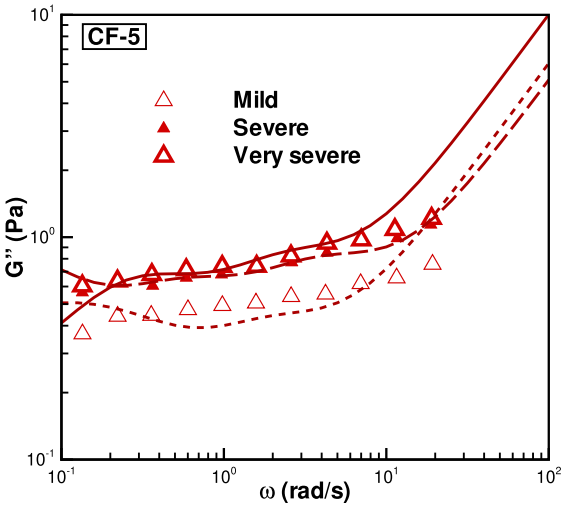

(b) BMP+_τ_p-model dissipation modulus G'' predictions in SAOS.

Fig. 14. BMP+_τ_p-model predictions in a frequency sweep in SAOS for CF-5 samples. Symbols: Experimental data from Tomaiuolo et al.[17] $R^2 = \{0.75, 0.93, 0.91\}$ corresponds to Mild, Severe and Very Severe samples, respectively.

(i) *On the BMP+_τ_p-model predictive capabilities* - The BMP+_τ_p rheological equation-of-state describes quantitatively the rheological response of all the mucus-sputum cases analysed[5,11,17,19,20], in the linear and incipient non-linear regime. Here, the BMP+_τ_p parameters extracted from the data fitting describe systematically the thixo-viscoelastoplastic rheological features of human mucus and sputum.

(ii) *On conventional rheological mucus-sputum features and its description using the BMP+_τ_p model* - The overall rheological behaviour of samples is quantitatively-captured with the BMP+_τ_p model, where apparent viscosity drops of four-to-six orders-of-magnitude are recorded, signalling an apparent yield stress as one of the main features of human sputum. On top of this, viscoelastic characteristic-time spectra plays a relevant role in sputum transient mechanical response, with relaxation times ranging from seconds to minutes, as reported experimentally[5,11,17,19,20]. Although the viscoelastic features seem to prevail in the mucus and sputum behaviour in most of the studied flow scenarios, there are relevant regime transitions that might be explained via the manifestation of thixotropic features; then, comparison between characteristic

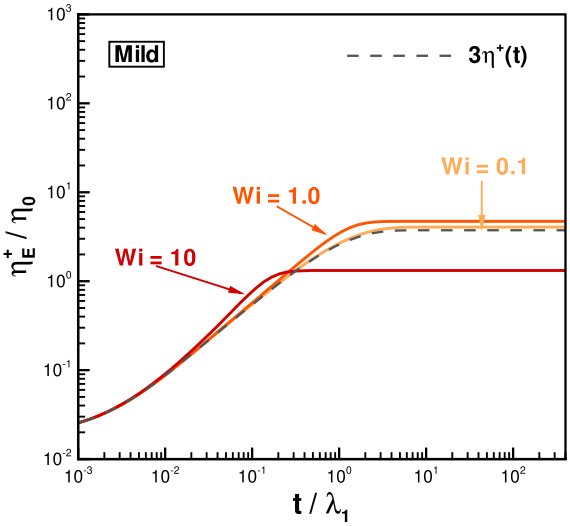

(a) Transient uniaxial extensional growth coefficient η_E^+ for the Mild CF-5 sample.

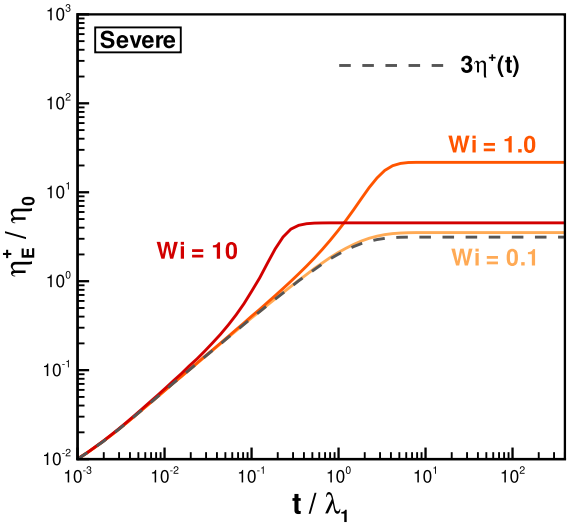

(b) Transient uniaxial extensional growth coefficient η_E^+ for the Severe CF-5 sample.

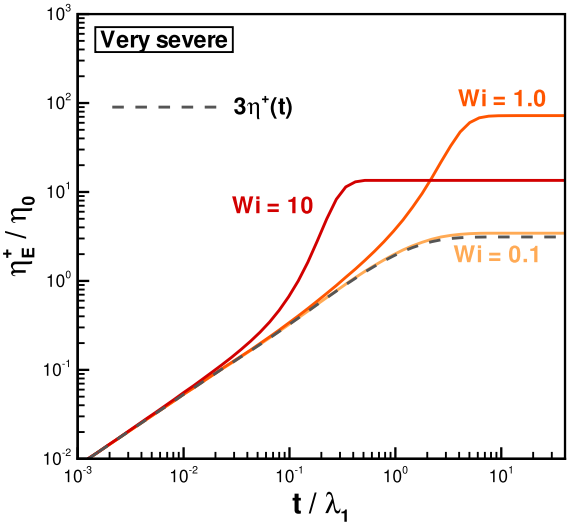

(c) Transient uniaxial extensional growth coefficient η_E^+ for the Very Severe CF-5 sample.

Fig. 15. BMP+_τ_p-model predictions for unsteady extensional flow (uniaxial elongation) for CF-5 samples for $Wi = \{0.1, 1, 10\}$. $Wi = \lambda_1 \dot{\epsilon}$ group-number definition is based in the extension-rate magnitude.

time scales associated to viscoelastic and thixotropic features could lead to find an actual hallmark for disease diagnosis and monitoring. In principle, this proposal could be extended to any other TVEP theoretical framework.

(iii) *On recently-observed thixotropic rheological mucus-sputum features and its description using the BMP+_τ_p model* - Evidence of thixotropy in healthy and ill-conditioned sputum samples has been reported in some works[11], a fact that the BMP+_τ_p model captures quantitatively as well, revealing an explicit relationship between the so-called critical stress for fluidisation τ_c (understood in rheology as a measure of yield stress) and the product of the BMP+_τ_p construction-destruction thixotropic parameters, which translates inversely into a characteristic rate of energy dissipation for fluid structure breakdown. Here, an explicitly-derived critical stress measure $\tau_c = \sqrt{\frac{\eta_\infty}{\lambda_s k_0}}$ is proposed and used to estimate a measure of a yield stress value of mucus-sputum. One should note that the BMP+_τ_p characteristic thixotropic energy-dissipation rate $(\frac{1}{\lambda_s \cdot k_0})$ appears explicit in such τ_c measure, rendering larger τ_c-values under diminishing $\lambda_s \cdot k_0$ products. Notably, the BMP+_τ_p τ_c-predictions concur quantitatively with independent experimentally-obtained τ_c-values[20].

(iv) *On BMP+_τ_p-model predictions of highly non-linear responses under LAOS and uniaxial extensional deformations* - Exploration by predictive modelling of the extensional features of human sputum reveal attractive features which correlate with the apparent thickening of mucus under CF infections. Particularly for CF severe conditions, sputum displays a marked extension hardening response at intermediate extension-rate, which might explain the *extra resistance* to mobilise sputum from the airways. The development of such extension hardening has a direct relationship with the rise of τ_c, the drop of the thixotropic $\lambda_s \cdot k_0$ product, and the development of secondary loops in Lissajous viscous projections under LAOS.

(v) *On more robust rheological characterisation protocols for biofluids* Our findings reveal the necessity of performing thorough experimental rheological characterisation of human sputum and mucus given the thixo-viscoelastoplastic nature of these type of biomaterials. As such, independent experimental tests should be implemented on sputum samples to reveal their time-dependent viscoelastic properties , such as steady simple shear and extension, and dynamic SAOS, LAOS and thixotropic loops. Here, although some studies have looked into a detailed rheological description of sputum,[5,11,17,19,20] the general practise is to look to basic steady simple shear flow and linear viscoelastic SAOS characterisation, thus providing limited information to be analysed theoretically in seek of a robust rheological characterisation and its connection to respiratory-system illnesses.

Remarkably, this study has driven us to conclude that it is not only viscoelasticity the determining factor of mucus and sputum health state. From this study, one of the main conclusions, withdrawn from a deep theoretical rheological characterisation with the BMP+_τ_p model, is that thixotropy, viscoelasticity, plasticity and banding properties in some instances, are also relevant for the general mechanical description of mucus-sputum, in contrast to previous studies in which a partial picture of those properties is displayed[5,11,17,19,20,43,47]. As such, through the mathematical modelling of mucus-sputum rheological response in healthy state and distinct types and degrees of pulmonary diseases (CF, COPD, COVID-19[5,9,11,17,19,20]), one can certainly look for complementary rheological signals that may help to develop more robust experimental protocols for characterising complex biofluid systems and soundly-based biomarkers in sight of their application in clinical practise with the help of medicine practitioners.

Data availability

The datasets used and/or analysed in this study are publicly available from the corresponding author on reasonable request.

Received: 29 December 2024; Accepted: 13 August 2025
Published online: 12 December 2025

References

1. Lai, S. K., Wang, Y.-Y., Wirtz, D. & Hanes, J. Micro-and macrorheology of mucus. *Adv. Drug Deliv. Rev.* **61**, 86–100. https://doi.org/10.1016/j.addr.2008.09.012 (2009).
2. Pangeni, R. et al. Airway mucus in pulmonary diseases: Muco-adhesive and muco-penetrating particles to overcome the airway mucus barriers. *Int. J. Pharm.* **634**, 122661. https://doi.org/10.1016/j.ijpharm.2023.122661 (2023).
3. Creeth, J. M. Constituents of mucus and its separation. *Br. Med. Bull.* **34**, 17–24. https://doi.org/10.1093/oxfordjournals.bmb.a071454 (1978).
4. Leal, J., Smyth, H. D. & Ghosh, D. Physicochemical properties of mucus and their impact on transmucosal drug delivery. *Int. J. Pharm.* **532**, 555–572. https://doi.org/10.1016/j.ijpharm.2017.09.018 (2017).
5. Dawson, M., Wirtz, D. & Hanes, J. Enhanced viscoelasticity of human cystic fibrotic sputum correlates with increasing microheterogeneity in particle transport. *J. Biol. Chem.* **278**, 50393–50401. https://doi.org/10.1074/jbc.M309026200 (2003).
6. Bansil, R. & Turner, B. S. The biology of mucus: Composition, synthesis and organization. *Adv. Drug Deliv. Rev.* **124**, 3–15. https://doi.org/10.1016/j.addr.2017.09.023 (2018).
7. Huck, B. C. et al. Macro-and microrheological properties of mucus surrogates in comparison to native intestinal and pulmonary mucus. *Biomacromolecules* **20**, 3504–3512. https://doi.org/10.1021/acs.biomac.9b00780 (2019).
8. Kavishvar, D. & Ramachandran, A. The yielding behaviour of human mucus. *Adv. Colloid Interface Sci.* 103049, https://doi.org/10.1016/j.cis.2023.103049 (2023).
9. Kratochvil, M. J. et al. Biochemical and biophysical characterization of respiratory secretions in severe sars-cov-2 (covid-19) infections. *Medrxiv: the Preprint Server for Health Sciences* 2020–09, https://doi.org/10.1172/jci.insight.152629 (2021).
10. Ichikawa, S., Matsumura, K., Erami, K. & Ito, S. Biological significance of the respiratory mucus rheology in mucociliary clearance. *Nihon Reoroji Gakkaishi* **51**, 105–110. https://doi.org/10.1678/rheology.51.105 (2023).
11. Nielsen, H., Hvidt, S., Sheils, C. A. & Janmey, P. A. Elastic contributions dominate the viscoelastic properties of sputum from cystic fibrosis patients. *Biophys. Chem.* **112**, 193–200. https://doi.org/10.1016/j.bpc.2004.07.019 (2004).
12. Puchelle, E. et al. Elasto-thixotropic properties of bronchial mucus and polymer analogs. *Biorheology* **22**, 415–423. https://doi.org/10.3233/bir-1985-22505 (1985).
13. Georgiades, P., Pudney, P. D., Thornton, D. J. & Waigh, T. A. Particle tracking microrheology of purified gastrointestinal mucins. *Biopolymers* **101**, 366–377 (2014).
14. Wagner, C., Wheeler, K. & Ribbeck, K. Mucins and their role in shaping the functions of mucus barriers. *Annu. Rev. Cell Dev. Biol.* **34**, 189–215 (2018).
15. Esteban Enjuto, L., Robert de Saint Vincent, M., Maurin, M., Degano, B. & Bodiguel, H. Sputum handling for rheology. *Sci. Rep.* **13**, 7695, https://doi.org/10.1038/s41598-023-34043-9 (2023).
16. Esteban Enjuto, L. et al. Rheological comparison of sputum and reconstituted airway epithelium mucus. *Sci. Rep.* **14**, 31660 (2024).
17. Tomaiuolo, G. et al. A new method to improve the clinical evaluation of cystic fibrosis patients by mucus viscoelastic properties. *PloS one* **9**, e82297. https://doi.org/10.1371/journal.pone.0082297 (2014).
18. Tabatabaei, S. et al. A caber computational-experimental rheological study on human sputum. *J. Non-Newton. Fluid Mech.* **222**, 272–287. https://doi.org/10.1016/j.jnnfm.2015.03.005 (2015).
19. Patarin, J. et al. Rheological analysis of sputum from patients with chronic bronchial diseases. *Sci. Rep.* **10**, 15685. https://doi.org/10.1038/s41598-020-72672-6 (2020).
20. Jory, M. et al. Mucus from human bronchial epithelial cultures: rheology and adhesion across length scales. *Interface Focus* **12**, 20220028. https://doi.org/10.1098/rsfs.2022.0028 (2022).

21. Puchelle, E., Zahm, J. & Quemada, D. Rheological properties controlling mucociliary frequency and respiratory mucus transport. *Biorheology* **24**, 557–563. https://doi.org/10.3233/BIR-1987-24606 (1987).
22. Nettle, C. et al. Linear rheology as a potential monitoring tool for sputum in patients with chronic obstructive pulmonary disease (copd). *Biorheology* **54**, 67–80. https://doi.org/10.3233/BIR-17141 (2018).
23. Fu, J. et al. Synovial fluid viscosity test is promising for the diagnosis of periprosthetic joint infection. *J. Arthroplasty* **34**, 1197–1200. https://doi.org/10.1016/j.arth.2019.02.009 (2019).
24. Bene, Z. et al. Laboratory biomarkers for lung disease severity and progression in cystic fibrosis. *Clin. Chim. Acta* **508**, 277–286. https://doi.org/10.1016/j.cca.2020.05.015 (2020).
25. Del Giudice, F. & Barnes, C. Rapid temperature-dependent rheological measurements of non-newtonian solutions using a machine-learning aided microfluidic rheometer. *Anal. Chem.* **94**, 3617–3628. https://doi.org/10.1021/acs.analchem.1c05208 (2022).
26. National Library of Medicine. National Center for Biotechnology Information. Sputum Analysis. https://www.ncbi.nlm.nih.gov/books/NBK563195/ (2023). Accessed: 11/23/24.
27. García, A. H., Moreno, D., Garmendia, J. V. & De Sanctis, J. B. Revisión de biomarcadores en asma y epoc. *Neumol Cir Torax* **72**, 299–305 (2013).
28. Stockley, R. A., Halpin, D. M., Celli, B. R. & Singh, D. Chronic obstructive pulmonary disease biomarkers and their interpretation. *Am. J. Respir. Crit. Care Med.* **199**, 1195–1204. https://doi.org/10.1164/rccm.201810-1860SO (2019).
29. Tabassum, T., Rahman, A., Araf, Y., Ullah, M. A. & Hosen, M. J. Prospective selected biomarkers in covid-19 diagnosis and treatment. *Biomark. Med.* **15**, 1435–1449. https://doi.org/10.2217/bmm-2021-0038 (2021).
30. World Health Organization. Chronic Obstructive Pulmonary Disease (COPD). https://www.who.int/health-topics/chronic-respiratory-diseases (2023). Accessed: 09/25/23.
31. World Health Organization (WHO). From emergency response to long-term COVID-19 disease management: sustaining gains made during the COVID-19 pandemic. https://www.who.int/publications/i/item/WHO-WHE-SPP-2023.1 (2023). Accessed: 11/23/24.
32. National Center for Biotechnology Information. Acute Respiratory Distress Syndrome. https://www.ncbi.nlm.nih.gov/books/NBK436002 (2023). Accessed: 09/25/23.
33. Marín, J. M. Viejos y nuevos criterios para clasificar la epoc. *Arch Bronconeumol* **40**, 9–15 (2004).
34. Hill, D. B. et al. A biophysical basis for mucus solids concentration as a candidate biomarker for airways disease. *PloS one* **9**, e87681. https://doi.org/10.1371/journal.pone.0087681 (2014).
35. Muhlebach, M. S. et al. Biomarkers for cystic fibrosis drug development. *J. Cyst. Fibros.* **15**, 714–723. https://doi.org/10.1016/j.jcf.2016.10.009 (2016).
36. Tzortzaki, E. G., Lambiri, I., Vlachaki, E. & Siafakas, N. M. Biomarkers in copd. *Curr. Med. Chem.* **14**, 1037–1048. https://doi.org/10.2174/092986707780362943 (2007).
37. O'Byrne, P. M. Exacerbations of asthma and copd: definitions, clinical manifestations and epidemiology. *Models of Exacerbations in Asthma and COPD* **14**, 1–11. https://doi.org/10.1159/000107049 (2007).
38. Broeckaert & Bernard. Clara cell secretory protein (cc16): characteristics and perspectives as lung peripheral biomarker. *Clin. Exp. Allergy* **30**, 469–475. https://doi.org/10.1046/j.1365-2222.2000.00760.x (2000).
39. Cazzola, M. & Novelli, G. Biomarkers in copd. *Pulm. Pharmacol. Ther.* **23**, 493–500. https://doi.org/10.1016/j.pupt.2010.05.001 (2010).
40. Fahy, J. V. & Dickey, B. F. Airway mucus function and dysfunction. *N. Engl. J. Med.* **363**, 2233–2247. https://doi.org/10.1056/NEJMra0910061 (2010).
41. Ghanem, R. et al. Apparent yield stress of sputum as a relevant biomarker in cystic fibrosis. *Cells* **10**, 3107. https://doi.org/10.3390/cells10113107 (2021).
42. Fulford, G. R. & Blake, J. R. Muco-ciliary transport in the lung. *J. Theor. Biol.* **121**, 381–402. https://doi.org/10.1016/S0022-5193(86)80098-4 (1986).
43. Sedaghat, M. H., Farnoud, A., Schmid, O. & Abouali, O. Nonlinear simulation of mucociliary clearance: a three-dimensional study. *J. Non-Newton. Fluid Mech.* **300**, 104727. https://doi.org/10.1016/j.jnnfm.2021.104727 (2022).
44. López-Aguilar, J. E. et al. A computational extensional rheology study of two biofluid systems. *Rheol. Acta* **54**, 287–305. https://doi.org/10.1007/s00397-014-0830-y (2015).
45. Levy, R., Hill, D. B., Forest, M. G. & Grotberg, J. B. Pulmonary fluid flow challenges for experimental and mathematical modeling. *Integr. Comp. Biol.* https://doi.org/10.1093/icb/icu107 (2014).
46. López-Aguilar, J. E., Webster, M. F., Tamaddon-Jahromi, H. R. & Manero, O. A new constitutive model for worm-like micellar systems-numerical simulation of confined contraction-expansion flows. *J. Non-Newton. Fluid Mech.* **204**, 7–21. https://doi.org/10.1016/j.jnnfm.2013.11.001 (2014).
47. Erken, O. et al. Effects of elastoviscoplastic properties of mucus on airway closure in healthy and pathological conditions. *Phys. Rev. Fluids* **8**, 053102. https://doi.org/10.48550/arXiv.2211.14352 (2023).
48. Saramito, P. A new constitutive equation for elastoviscoplastic fluid flows. *J. Non-Newton. Fluid Mech.* **145**, 1–14. https://doi.org/10.1016/j.jnnfm.2007.04.004 (2007).
49. Saramito, P. A new elastoviscoplastic model based on the herschel-bulkley viscoplastic model. *J. Non-Newton. Fluid Mech.* **158**, 154–161. https://doi.org/10.1016/j.jnnfm.2008.12.001 (2009).
50. Vasquez, P. A., Jin, Y., Palmer, E., Hill, D. & Forest, M. G. Modeling and simulation of mucus flow in human bronchial epithelial cell cultures-part i: Idealized axisymmetric swirling flow. *PLoS Comput. Biol.* **12**, e1004872. https://doi.org/10.1371/journal.pcbi.1004872 (2016).
51. Feather, E. & Russell, G. Sputum viscosity and pulmonary function in cystic fibrosis. *Arch. Dis. Child.* **45**, 807. https://doi.org/10.1136/adc.45.244.807 (1970).
52. Duangnumsawang, Y., Zentek, J. & Goodarzi Boroojeni, F. Development and functional properties of intestinal mucus layer in poultry. *Front. Immunol.* **12**, 745849. https://doi.org/10.3389/fimmu.2021.745849 (2021).
53. Ellingham, R. B., Berry, M., Stevenson, D. & Corfield, A. P. Secreted human conjunctival mucus contains muc5ac glycoforms. *Glycobiology* **9**, 1181–1189. https://doi.org/10.1093/glycob/9.11.1181 (1999).
54. McKinley, S. A. et al. Modeling neutralization kinetics of hiv by broadly neutralizing monoclonal antibodies in genital secretions coating the cervicovaginal mucosa. *PloS one* **9**, e100598. https://doi.org/10.1371/journal.pone.0100598 (2014).
55. Ren, S. et al. Numerical analysis of airway mucus clearance effectiveness using assisted coughing techniques. *Sci. Rep.* **10**, 2030. https://doi.org/10.1038/s41598-020-58922-7 (2020).
56. López-Aguilar, J. E., Webster, M. F., Tamaddon-Jahromi, H. R. & Manero, O. Predictions for circular contraction-expansion flows with viscoelastoplastic & thixotropic fluids. *J. Non-Newton. Fluid Mech.* **261**, 188–210. https://doi.org/10.1016/j.jnnfm.2018.09.001 (2018).
57. Lopez-Aguilar, J. E., Resendiz-Tolentino, O., Tamaddon-Jahromi, H. R., Ellero, M. & Manero, O. Flow past a sphere: Numerical predictions of thixo-viscoelastoplastic wormlike micellar solutions. *J. Non-Newton. Fluid Mech.* **309**, 104902. https://doi.org/10.1016/j.jnnfm.2022.104902 (2022).
58. López-Aguilar, J. E., Tamaddon-Jahromi, H. R. & Manero, O. Shear banding predictions for wormlike micellar systems under a contraction–expansion complex flow. *Phys. Fluids* **35**, https://doi.org/10.1063/5.0143432 (2023).
59. Walters, K. *Rheology* Vol. 1 (Chapman and Hall, London, 1975).

60. Morrison, F. A. et al. *Understanding rheology* Vol. 1 (Oxford University Press, New York, 2001).
61. Ewoldt, R. H., Hosoi, A. & McKinley, G. H. New measures for characterizing nonlinear viscoelasticity in large amplitude oscillatory shear. *J. Rheol.* **52**, 1427–1458. https://doi.org/10.1122/1.2970095 (2008).
62. Hyun, K. et al. A review of nonlinear oscillatory shear tests: Analysis and application of large amplitude oscillatory shear (laos). *Prog. Polym. Sci.* **36**, 1697–1753. https://doi.org/10.1016/j.progpolymsci.2011.02.002 (2011).
63. Rogers, S. A. & Lettinga, M. P. A sequence of physical processes determined and quantified in large-amplitude oscillatory shear (laos): Application to theoretical nonlinear models. *J. Rheol.* **56**, 1–25. https://doi.org/10.1122/1.3662962 (2012).
64. Rogers, S. A. In search of physical meaning: Defining transient parameters for nonlinear viscoelasticity. *Rheol. Acta* **56**, 501–525. https://doi.org/10.1007/s00397-017-1008-1 (2017).
65. Ahmad, M., Ritzoulis, C. & Chen, J. Shear and extensional rheological characterisation of mucin solutions. *Colloids Surf. B: Biointerfaces* **171**, 614–621 (2018).
66. Haward, S. J., Odell, J. A., Berry, M. & Hall, T. Extensional rheology of human saliva. *Rheol. Acta* **50**, 869–879 (2011).
67. Hu, Y., Romanò, F. & Grotberg, J. B. Effects of surface tension and yield stress on mucus plug rupture: a numerical study. *J. Biomech. Eng.* **142**, 061007 (2020).
68. Romano, F., Muradoglu, M., Fujioka, H. & Grotberg, J. The effect of viscoelasticity in an airway closure model. *J. Fluid Mech.* **913**, A31 (2021).
69. Malkin, A. Y., Derkach, S. R. & Kulichikhin, V. G. Rheology of gels and yielding liquids. *Gels* **9**, 715. https://doi.org/10.3390/gels9090715 (2023).
70. Hyun, K., Kim, S. H., Ahn, K. H. & Lee, S. J. Large amplitude oscillatory shear as a way to classify the complex fluids. *J. Non-Newton. Fluid Mech.* **107**, 51–65. https://doi.org/10.1016/S0377-0257(02)00141-6 (2002).
71. Dinkgreve, M., Paredes, J., Denn, M. M. & Bonn, D. On different ways of measuring "the" yield stress. *J. Non-Newton. Fluid Mech.* **238**, 233–241. https://doi.org/10.1016/j.jnnfm.2016.11.001 (2016).
72. Mewis, J. & Wagner, N. J. Thixotropy. *Adv. Colloid Interface Sci.* **147**, 214–227. https://doi.org/10.1016/j.cis.2008.09.005 (2009).
73. Larson, R. G. & Wei, Y. A review of thixotropy and its rheological modeling. *J. Rheol.* **63**, 477–501. https://doi.org/10.1122/1.5055031 (2019).
74. Bautista, F., De Santos, J., Puig, J. & Manero, O. Understanding thixotropic and antithixotropic behavior of viscoelastic micellar solutions and liquid crystalline dispersions. i. the model. *J. Non-Newton. Fluid Mech.* **80**, 93–113. https://doi.org/10.1016/S0377-0257(98)00081-0 (1999).
75. Garcia-Beristain, I. et al. Numerical simulations of thixotropic semi-solid aluminium alloys in open-rotor and rotor-stator mixers. *J. Non-Newton. Fluid Mech.* **321**, 105128. https://doi.org/10.1016/j.jnnfm.2023.105128 (2023).
76. Manero, O., Bautista, F., Soltero, J. & Puig, J. Dynamics of worm-like micelles: the cox-merz rule. *J. Non-Newton. Fluid Mech.* **106**, 1–15. https://doi.org/10.1016/S0377-0257(02)00082-4 (2002).
77. Moreno, L. et al. Effect of cholesterol and triglycerides levels on the rheological behavior of human blood. *Korea-Australia Rheology Journal* **27**, 1–10. https://doi.org/10.1007/s13367-015-0001-4 (2015).
78. Hill, D. B., Button, B., Rubinstein, M. & Boucher, R. C. Physiology and pathophysiology of human airway mucus. *Physiol. Rev.* **102**, 1757–1836 (2022).
79. Barnes, H. A. The yield stress-a review or '$\pi\alpha\nu\tau\alpha\rho\varepsilon\iota$'-everything flows?. *J. Non-Newton. Fluid Mech.* **81**, 133–178 (1999).
80. Lafforgue, O., Seyssiecq, I., Poncet, S. & Favier, J. Rheological properties of synthetic mucus for airway clearance. *J. Biomed. Mater. Res. A* **106**, 386–396. https://doi.org/10.1002/jbm.a.36251 (2018).
81. Lele, A. & Mashelkar, R. Energetically crosslinked transient network (ectn) model: implications in transient shear and elongation flows. *J. Non-Newton. Fluid Mech.* **75**, 99–115. https://doi.org/10.1016/S0377-0257(97)00070-0 (1998).
82. Islam, M. T. Prediction of multiple overshoots in shear stress during fast flows of bidisperse polymer melts. *Rheol. Acta* **45**, 1003–1009. https://doi.org/10.1007/s00397-005-0060-4 (2006).
83. Varchanis, S., Makrigiorgos, G., Moschopoulos, P., Dimakopoulos, Y. & Tsamopoulos, J. Modeling the rheology of thixotropic elasto-visco-plastic materials. *J. Rheol.* **63**, 609–639. https://doi.org/10.1122/1.5049136 (2019).
84. Stickel, J. J., Knutsen, J. S. & Liberatore, M. W. Response of elastoviscoplastic materials to large amplitude oscillatory shear flow in the parallel-plate and cylindrical-couette geometries. *J. Rheol.* **57**, 1569–1596. https://doi.org/10.1122/1.4820495 (2013).
85. Ewoldt, R. H. & McKinley, G. H. On secondary loops in laos via self-intersection of lissajous-bowditch curves. *Rheol. Acta* **49**, 213–219. https://doi.org/10.1007/s00397-009-0408-2 (2010).
86. Ewoldt, R. H. & McKinley, G. H. Mapping thixo-elasto-visco-plastic behavior. *Rheol. Acta* **56**, 195–210. https://doi.org/10.1007/s00397-017-1001-8 (2017).
87. Pino-Argumedo, M. I. et al. Elastic mucus strands impair mucociliary clearance in cystic fibrosis pigs. *Proc. Natl. Acad. Sci.* **119**, e2121731119 (2022).

Acknowledgements

J.E.L.-A. acknowledges the support from Secretaría de Ciencia, Humanidades, Tecnología e Innovación (SECIHTI - Ex-CONAHCYT, Mexico - grant number CF-2023-I-318) and from Universidad Nacional Autónoma de México UNAM (grant numbers PAPIIT IN106424, PAPIME PE103125 and PAIP 5000-9172 Facultad de Química). J.E.L.-A. and O.M. acknowledge the support from UNAM under the project with Grant No. PAPIIT IN100623. M.F.-L. and S.L.E.-C. acknowledge the support from Secretaría de Ciencia, Humanidades, Tecnología e Innovación (SECIHTI - Ex-CONAHCYT), for the scholarships (CVU numbers 1147394 and 2058269, respectively) to fund their post-graduate studies.

Author contributions

J.E.L.-A. and M.F.-L. conceptualised this research work. M.F.-L. and J.E.L.-A. developed the methodology. M.F.-L. and J.E.L.-A. developed the software. All authors validated the results. All authors performed the formal analysis of data and performed a thorough literature investigation. J.E.L.-A. provided the resources. M.F.-L., S.L.E.-C., M.F.R.-T. and J.E.L.-A. curated the data. M.F.-L. and J.E.L.-A. prepared and wrote the original draft. All authors reviewed and wrote the manuscript. J.E.L.-A. was responsible for the project administration. J.E.L.-A. and O.M. were responsible for funding acquisition.

Declarations

Competing interests

The authors declare no competing interests.

Additional information

Supplementary Information The online version contains supplementary material available at https://doi.org/10.1038/s41598-025-16178-z.

Correspondence and requests for materials should be addressed to J.E.L.-A.

Reprints and permissions information is available at www.nature.com/reprints.

Publisher's note Springer Nature remains neutral with regard to jurisdictional claims in published maps and institutional affiliations.